FATIGUE DAMAGE TO STEEL BRIDGE DIAPHRAGMS, FIELD INVESTIGATION

By

LIM, KEE SEONG

Bachelor of Science in Civil Engineering

Oklahoma State University

Stillwater, Oklahoma

1987

Submitted to the Faculty of the
Graduate College of the
Oklahoma State University
in partial fulfillment of
the requirements for
the Degree of
MASTER OF SCIENCE
May, 1989

FATIGUE DAMAGE TO STEEL BRIDGE DIAPHRAGMS,

FIELD INVESTIGATION

Thesis Approved:

Thesis Adviser

Dean of Graduate College

ACKNOWLEDGMENTS

I would like to express my sincere thanks, appreciation and gratitude to my advisor, Dr. Farrel Zwerneman for his original ideas, guidance and support, which was the backbone of the success of this study.

Special thanks are extended to the ODOT personnel who provided the necessary facilities and help in the field investigation.

To my friends and colleagues who have provided me with their warm friendship, good times, and help during the course of my educational experience in Oklahoma State University, I owe them my gratitude and appreciation.

Finally, I dedicate this thesis to my parents for their continual support, encouragement and love.

TABLE OF CONTENTS

Chapter		Page
I.	INTRODUCTION	1
	1.1 Problem Statement	1
	1.2 Objectives of Study	1
	1.3 Background	2
II.	LITERATURE REVIEW	8
	2.1 Wheel Load Distribution on Beam and Slab Highway Bridges	8
	2.2 Fatigue Damage in Bridges	11
	2.3 Problem with Distortion and Restraint of Simple End Connection Components	11
	2.4 Fatigue Problems Due to Initial Discontinuities and Residual Stresses	14
	2.5 Problem Due to Poor Details	15
III.	METHODS	17
	3.1 Load Testing in Field	17
	3.2 Analytical Models	26
	3.3 Laboratory Tests	30
IV.	RESULTS	33
	4.1 Results from Field Measurements and Grid Model	33
	4.2 Finite Element Analysis	42
	4.3 Mechanical and Chemical Properties	42
	4.4 Discussion of Results	46
	4.5 Recommendations	50
V.	SUMMARY AND CONCLUSIONS	52
	5.1 Summary	52
	5.2 Conclusion	53
BIBLIOGRAPHY		54

Chapter Page

APPENDIX 57

LIST OF TABLES

Table		Page
I.	Position of truck versus distance along bridge	25
II.	Chemical properties of wide flange	45
III.	Data from Charpy impact tests	47
IV.	Strain versus depth of diaphragm	58
V.	Strain versus positions of truck for gage #22, laboratory instrumented diaphragm	59
VI.	Strain versus positions of truck for field instrumented exterior diaphragm, gage #8	60
VII.	Calculated displacement versus distance along bridge for the interior girder	61
VIII.	Calculated stress versus distance from bottom cope	62

LIST OF FIGURES

Figure		Page
1.	Plan view of diaphragms and stringers	3
2.	Typical diaphragm framing and crack pattern	4
3.	Fractured diaphragm with 100% section loss	5
4.	Diaphragm showing small crack at coped section ...	6
5.	Cracked web at simple stringer end connection	13
6.	Location of laboratory and field instrumented strain gage diaphragms	18
7.	Location of strain gages on laboratory instrumented diaphragm	19
8.	Location of strain gages on field instrumented interior diaphragm	20
9.	Location of strain gages on field instrumented exterior diaphragm	21
10.	Tank truck used for loading bridge	22
11.	Lane loadings at various positions along first three spans of bridge	23
12.	Shoulder Loadings at various positions along first three spans of bridge	24
13.	Grid model of first three spans of bridge	27
14.	Finite element model for diaphragm with coped bottom flange	28
15.	Magnified view of the finite element model near the coped flange	29
16.	Uncoped diaphragm	31
17.	Diaphragm with tapered cope	32

Figure Page

18. Strains for various shoulder loading positions, laboratory instrumented diaphragm, gage #22 34

19. Strains for various lane loading positions, field instrumented exterior diaphragm, gage #8 35

20. Unscaled plot of strain versus time for different truck speeds 37

21. Strain versus depth for laboratory instrumented diaphragm, gages #1,#4,#7, loading at position 5 38

22. Strain versus depth for laboratory instrumented diaphragm, gages #1,#4,#7, loading at position 29 39

23. Strain versus depth for laboratory instrumented diaphragm, gages #10,#13, loading at position 5 40

24. Strain versus depth for laboratory instrumented diaphragm, gages #10,#13, loading at position 29 41

25. Deflected shape of an interior girder obtained using the grid model, loading at position 5 43

26. Stress along crack line from finite element models 44

27. Charpy impact test data for beam flange 48

28. Charpy impact test data for beam web 49

29. Strains for various shoulder loading positions, laboratory instrumented diaphragm, gage #0 64

30. Strains for various lane loading positions, laboratory instrumented diaphragm, gage #2 65

31. Strains for various lane loading positions, field instrumented exterior diaphragm, gage #3 66

32. Deflected shape of the center girder obtained using the grid model, loading at position 5 67

33. Stress versus strain curve for flange specimen 1 . 68

Figure Page

34. Stress versus strain curve for flange specimen 2 . 69

35. Stress versus strain curve for web specimen 1 70

36. Stress versus strain curve for web specimen 2 71

CHAPTER I

INTRODUCTION

1.1 Problem Statement

This research was conducted to identify the cause of diaphragm cracking in a steel girder highway bridge. The bridge used in this research is located on Interstate 40 near Weatherford, Oklahoma. The bridge is about 20 years old and 60 of the 184 diaphragms in the bridge are cracked. The components of this research include a literature search, load testing of the bridge, and analyses of the bridge superstructure and diaphragms. The final part of this research, which is not part of this report, involves the testing of diaphragms in the laboratory.

1.2 Objectives of Study

The objective of this research is to determine the cause of diaphragm cracking in the subject bridge. Once the cause has been identified, the problem can be corrected and the likelihood of the same problem occurring in other bridges can be assessed. A better understanding of the cause of diaphragm cracking in the subject bridge will also help reduce the possibility of the same problem occurring in future construction.

1.3 Background

During a routine inspection, an Oklahoma Department of Transportation (ODOT) inspector found several fractured diaphragms on a steel girder highway bridge on Interstate 40 near Weatherford, Oklahoma. A follow-up inspection revealed that about 33 percent of the diaphragms on both the westbound and eastbound spans were cracked (Fig 1). All the cracks were found to originate at flange copes. In five cases diaphragms suffered 100% section loss. Typical crack patterns are shown in Figures 2, 3, and 4.

To determine the cause of cracking in the diaphragms, ODOT engineers performed a computer aided structural analysis. They found that the diaphragm-to-longitudinal-member connection is capable of supporting a significant moment. It was hypothesized that the high moment capacity of this connection causes the four individual diaphragms across the bridge to act as a continuous member. When the bridge is loaded by the passage of a vehicle, the interior longitudinal members are more heavily loaded than the exterior members. This causes the interior longitudinal members to deflect more than the exterior members. The 'continuous' diaphragms are loaded by these differential deflections of the longitudinal members, resulting in tension along the bottom of the diaphragms.

This hypothesis is supported by the crack patterns on the diaphragms in the bridge (Figs 2,3,4). In general, the cracks originate in the bottom flange cope and do not

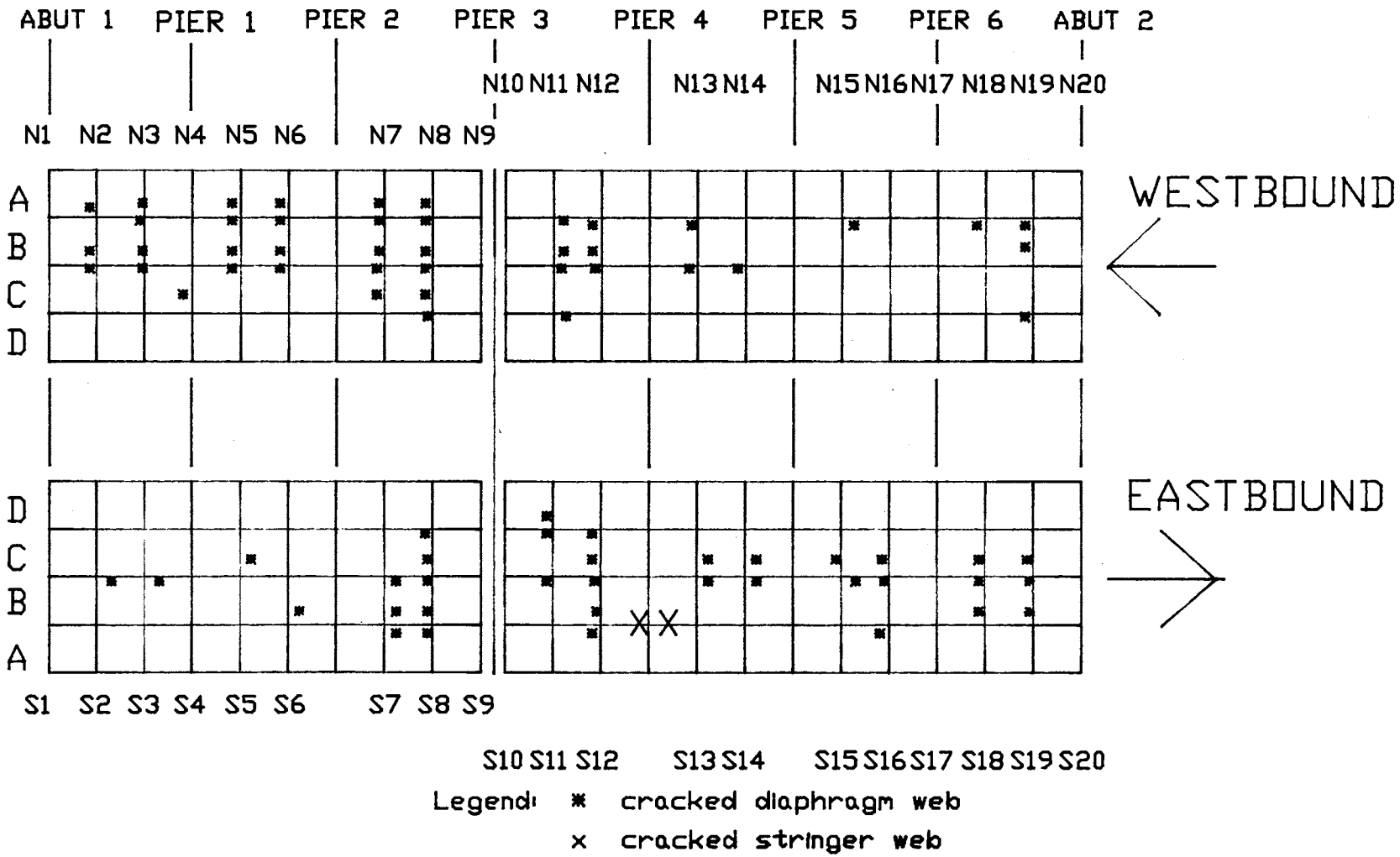

Figure 1. Plan view of diaphragms and stringers

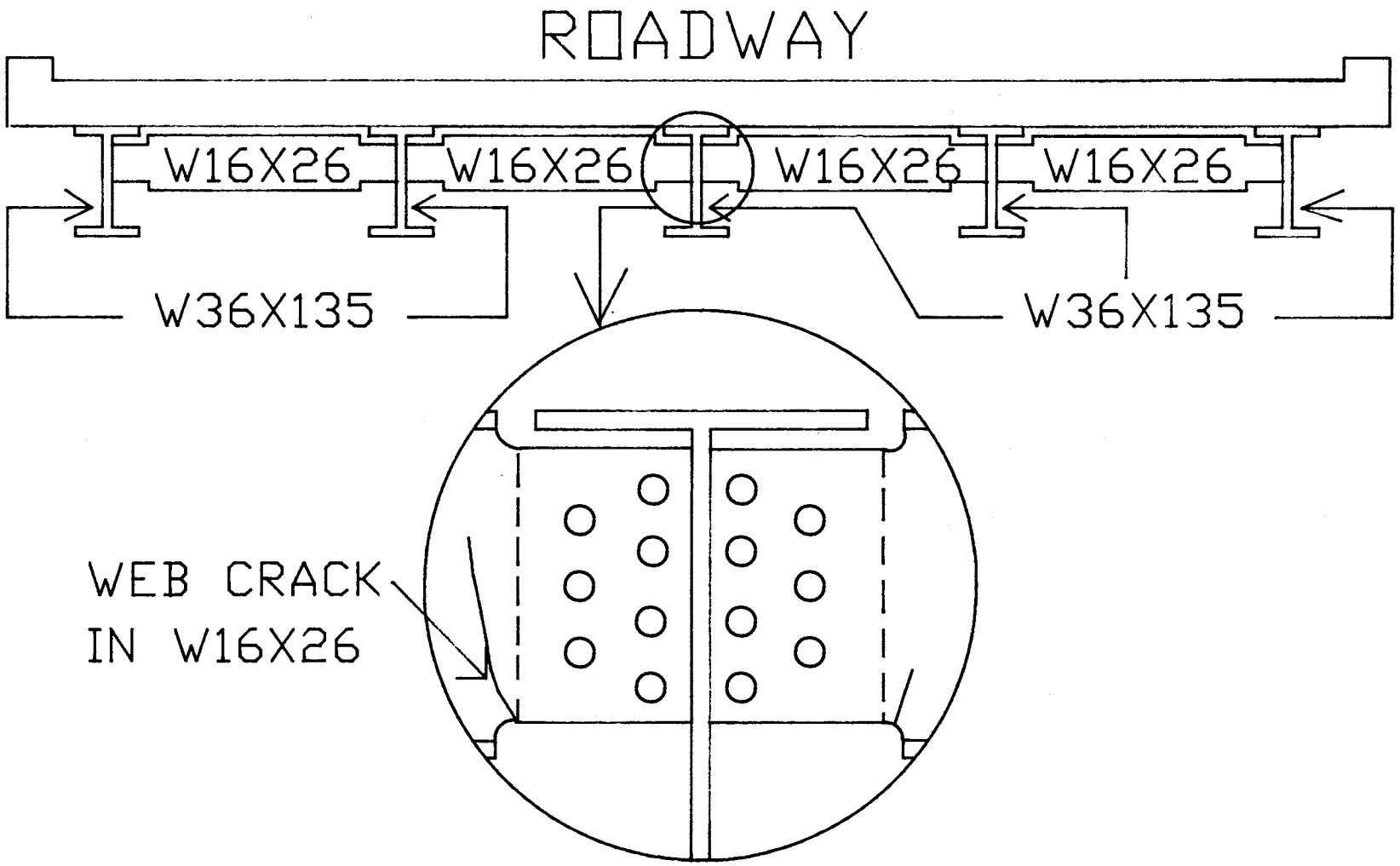

Figure 2. Typical diaphragm framing and crack pattern

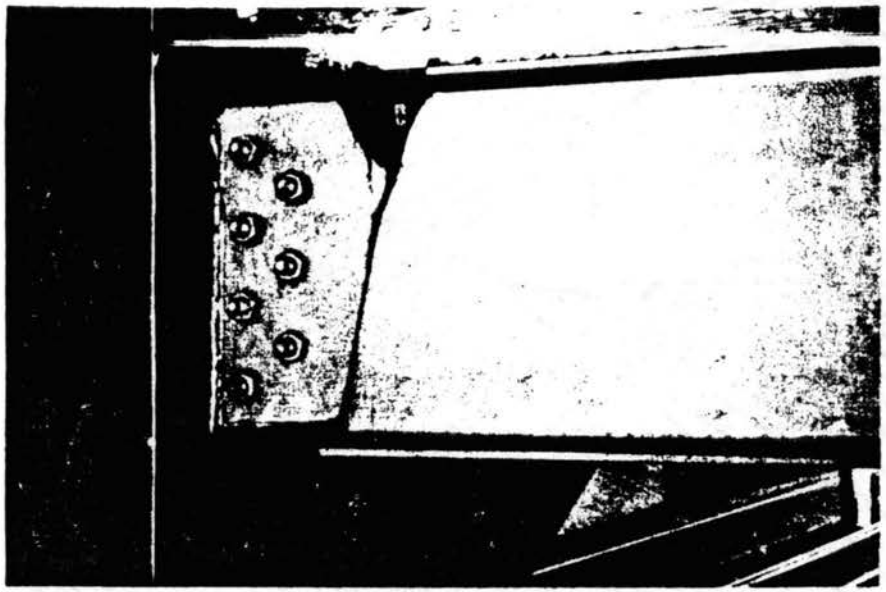

Figure 3. Fractured diaphragm with 100% section loss

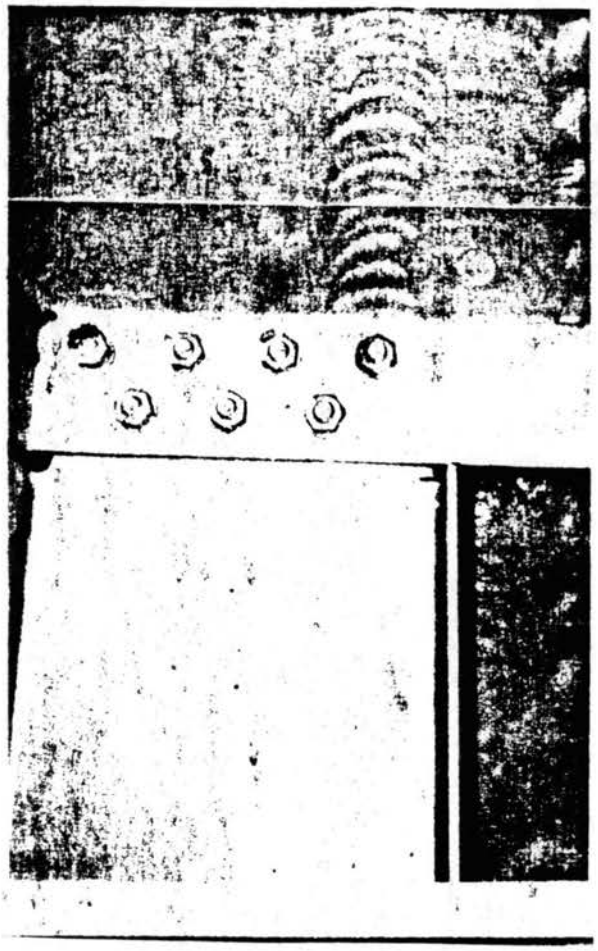

Figure 4. Diaphragm showing small crack at coped section

occur in diaphragms located immediately over a concrete pier cap. In the one case where cracks were found in diaphragms over a concrete pier cap, the cracks originate at the top of the diaphragm. These observations indicate that at points far away from the pier cap, where the longitudinal members are relatively free to deflect independently, the bottom of the diaphragms are in tension. Diaphragms directly above the pier cap appear to be loaded by forces passing through the concrete slab directly into the diaphragms. The longitudinal members over the pier cap are not free to deflect, and act as fixed supports for the diaphragms, producing negative moment at the diaphragm ends.

Another important feature in the pattern of cracked diaphragms is the lack of cracks in diaphragm ends connected to exterior girders. This indicates that maximum moment occurs in the interior diaphragms. Apparently, the exterior girders away from concrete pier caps are flexible enough torsionally to prevent the development of significant negative moment in the diaphragms.

Tension in the bottom flange cope is magnified by the stress concentration at the cope. Residual stress induced by flame cutting also adds to the stress. The end result is stress of sufficient magnitude at the cope to initiate and propagate fatigue cracks.

CHAPTER II

LITERATURE REVIEW

2.1 Wheel Load Distribution on Beam and Slab Highway Bridges

Current AASHTO specifications allow the use of a simplified analysis for bridge superstructures. Wheel load distribution factors are tabulated for most types of beam and slab bridges (4). Bridge engineers typically treat the deck and multi-girder structure as a beam. Total moment is distributed to the interior and exterior girders according to a design factor. The design factor is given by

$$g = s/d$$

where g = a fraction of a wheel load as tabulated in AASHTO codes;

s = center to center girder spacing; and

d = a constant depending on the bridge type and number of loaded lanes.

Wheel loads for end shear are distributed by assuming the flooring to act as a simple span between girders.

Loads derived in this way are used to design the bridge for strength. Loads of this magnitude do not occur frequently enough to affect the fatigue life of a bridge. For instance, for the design of a continuous span bridge

governed by lane loading, the loading is first applied over certain positions of the bridge to obtain the maximum possible positive moment and then over other portions of the bridge to obtain the maximum negative moment. Summing these moments results in a large stress range, but this stress range would occur only rarely. Thus, it is overconservative for use in determining the fatigue life of a bridge.

AASHTO requires that members and connections that are subjected to variations and reversals of stress be designed against fatigue failure. Lower s/d factors (based on a truck on only one lane) could be used for fatigue design as compared to static design (9). These lower factors are based on results from field measurements and theoretical calculations.

Numerous field measurements (5,16) have shown that the actual stresses occurring in longitudinal beams and stringers in bridges under traffic are much smaller than those calculated using AASHTO methods. Ghosn, Michael, et al.(16) used results from a weigh-in-motion system to evaluate bridges. They found that distribution factors were typically lower than prescribed in AASHTO specifications. Actual measurements of the distribution of a single vehicle in a single lane were used in the calculation of girder distribution factors. To account for multiple truck loadings, results of distribution factors from adjacent lane loadings are combined. Field measurements (5) showed that the average lateral distribution factor was s/14.7 for the

10 bridges measured. AASHTO specifies a lateral distribution factor of s/5.5 for these type bridges.

Besides field investigations, numerous theoretical calculations (17,19,22,24,25) on wheel load distribution have been carried out. William H. Walker (25) used three analytical models for his study. Bridge and deck structural idealizations were done using 1) an "exact" idealization using shell bending elements with axial membrane forces placed eccentric to the girders and diaphragm elements; 2) a grid idealization using plate bending elements; and 3) a simple grid in which both transverse and longitudinal effects of deck-girder composite action were taken into account. A comparison of the results of these three models was made. It was found that the results from the simple grid model are in close agreement with the other two more "exact" models.

The simple grid model was created using transverse beams to represent the equivalent slab and diaphragms (if present) and using longitudinal girders to model the composite moment of inertia for longitudinal bending. Analysis results revealed that the AASHTO specification overestimates both the interior beam moment and the edge girder moment. Other studies (17,19) using finite element models provided similar results.

2.2 Fatigue Damage in Bridges

Fatigue may be defined as the initiation and propagation of microscopic cracks into macroscopic cracks under cyclic loads. If macroscopic cracks are allowed to increase in size, the effective cross-sectional area will be reduced. Structural failures of members will result when applied stresses are large enough to cause yielding or fracture of the members.

Fatigue has been a constant problem in bridges. Between 1978 and 1981, a survey was carried out to gather information on fatigue cracking in bridges (6). This survey covered 142 bridge sites in twenty states plus Ontario, Canada. It was determined that cracking patterns could be grouped into general categories.

2.3 Problem with Distortion and Restraint of Simple End Connection Components

Many bridge sites developed fatigue cracks under the category of out-of-plane distortion. These types of cracks usually involved a segment of the girder web. Often a large number of cracks are found when fatigue cracks develop as a result of out-of-plane distortion.

Framing connections that fasten beams or girder ends are often considered flexible enough to carry shear only. In practice, however, bolted and welded connections

are not completely free to rotate. There is always some end restraint to resist the end rotation of the beam. This end rotation will cause the connections to distort. Distortion in small gaps (distance between the bottom of the top flange and the connection plates) causes high cyclic stress amplitude, thus forming cracks in the structural system.

Cracks can also develop in the "simply supported" beam. In most static loading cases, the development of restraint is considered to be beneficial as it increases the resisting capacities of the members. Under cyclic loading, however, this restraint can cause fatigue damage and cracking to the connected parts (12,13). An example of this is a stringer which was coped at the bottom flange to provide clearance for a floor beam flange (Fig 5). This stringer was bolted with a "simple" web angle connection to the floor beam. A crack developed at the coped end of the flange.

Because of the cope, the bending stress range was found to be three times greater than it would have been if there were no cope. Cracking occurs because these stringers act as 'continuous' members. The differential deflections of the floor beams cause the coped flange to experience tension during part of the stress cycle. This tension was magnified by the stress concentration at the cope and by the residual stress caused by flame cutting. When the crack has propagated through the zone of residual tensile stress, the end shear and restraining moment are large enough to continue propagating the crack.

Figure 5. Cracked web at simple stringer end connection (13)

Diaphragms and cross frames are secondary members which are frequently used in multiple beam bridges. The main reason for their use is to help distribute loads laterally in the structural system. As the structure is loaded, the longitudinal girders deform differentially at the cross sections where the diaphragms and cross frames are installed. When this happens, the girder webs can be displaced out-of-plane by the secondary members. The magnitude of out-of-plane web displacement is dependent upon the relative magnitudes of the girder displacements and the lateral bending resistance of the girder flange. This out-of-plane displacement will cause tensile stresses to occur in the girder web, and when loaded cyclically to a sufficient magnitude, fatigue cracks will initiate and propagate (13).

2.4 Fatigue Problems Due to Initial Discontinuities and Residual Stresses

Initial defects and discontinuities in welded members and components is another fatigue crack category. All welding processes introduce discontinuities in or near the weldment. These internal discontinuities could be due to porosity (gas pockets), incomplete fusion, or trapped slag. When the weld shrinks upon cooling, residual tensile stresses develop in the weldment and the base metal adjacent to it. These residual tensile stresses are at or near the

yield point. Hence, in most welded structures, the initial stages of fatigue crack growth occur in weldments (7,8,9,10,11,12,13,14). Poor quality welding is one of the major causes of this fatigue condition.

Under cyclic loading, the material at or near the initial discontinuity will be subjected to a full tension cycle, even in cases of nominal compression. Researchers have noted the presence of fatigue cracks growing in the web-flange intersection on the compression side of a beam (7). The cracks were arrested after they grew out of the residual tensile stress field and they did not impair the load carrying capacity of the member. However, when the applied loading produces a tension-tension stress cycle, the fatigue crack propagation can be quite severe. The higher the applied stress range and the larger the initial flaw, the faster the fatigue crack propagates.

2.5 Problem Due to Poor Details

Another fatigue category is made up of members and components which crack as a result of poor fatigue details. A poor fatigue detail generally involves a dramatic change in member geometry in a high tensile stress area. This change in geometry results in a high stress concentration factor. An example of poor fatigue details is shown in Figure 5. When the bottom flange of the stringer was loaded in tension, the poor details due to the cope at the bottom flange magnified the stress concentration at the coped

section. Residual tensile stresses due to flame cutting adds to this stress. Because of the poor details, crack growth was found to occur at the bottom flange cope.

CHAPTER III

METHODS

3.1 Load Testing in Field

This portion of the research involves the measurement of strains in diaphragms while the bridge is supporting a known load. A diaphragm fabricated to match the existing diaphragms was instrumented with strain gages at the Oklahoma State University Structural Laboratory. Laboratory installation of strain gages was considered since it allows more accurate positioning and reduces the possibility of bad gages. The instrumented diaphragm from the laboratory was used to replace the cracked diaphragm D2 as shown in Figure 6. Details of the laboratory instrumented diaphragm are shown in Figure 7. Two other uncracked diaphragms D1 and D3 were instrumented in the field (Fig 6) to provide additional data. The details of these diaphragms are shown in Figures 8 and 9. Measurement of differential displacements of longitudinal members in vertical and horizontal directions was also attempted during the field investigations, but was not successful.

The bridge was loaded with a tank truck supplied by ODOT (Fig 10). Strain measurements were taken for both lane and shoulder loading conditions (Figs 11,12). Table I

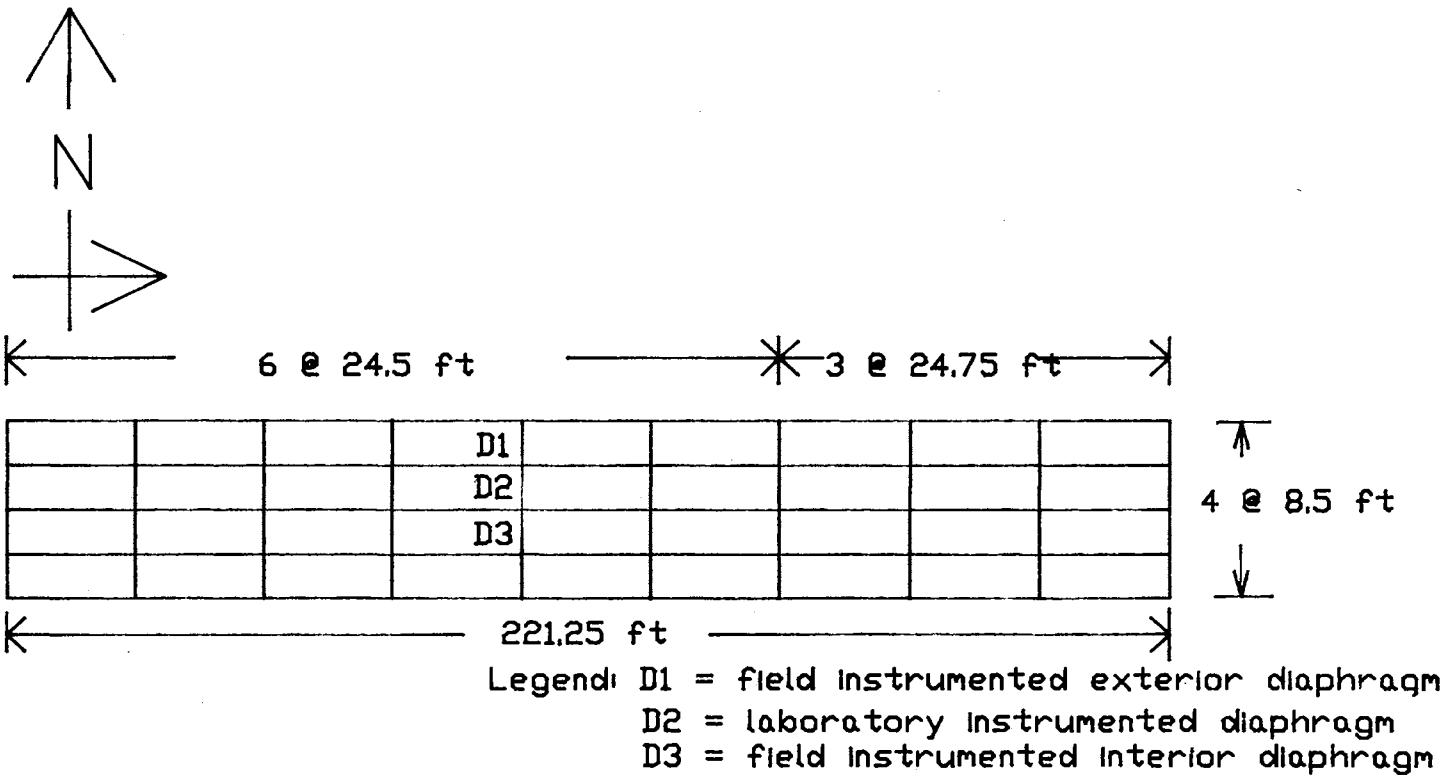

Figure 6. Location of laboratory and field instrumented strain gage diaphragms

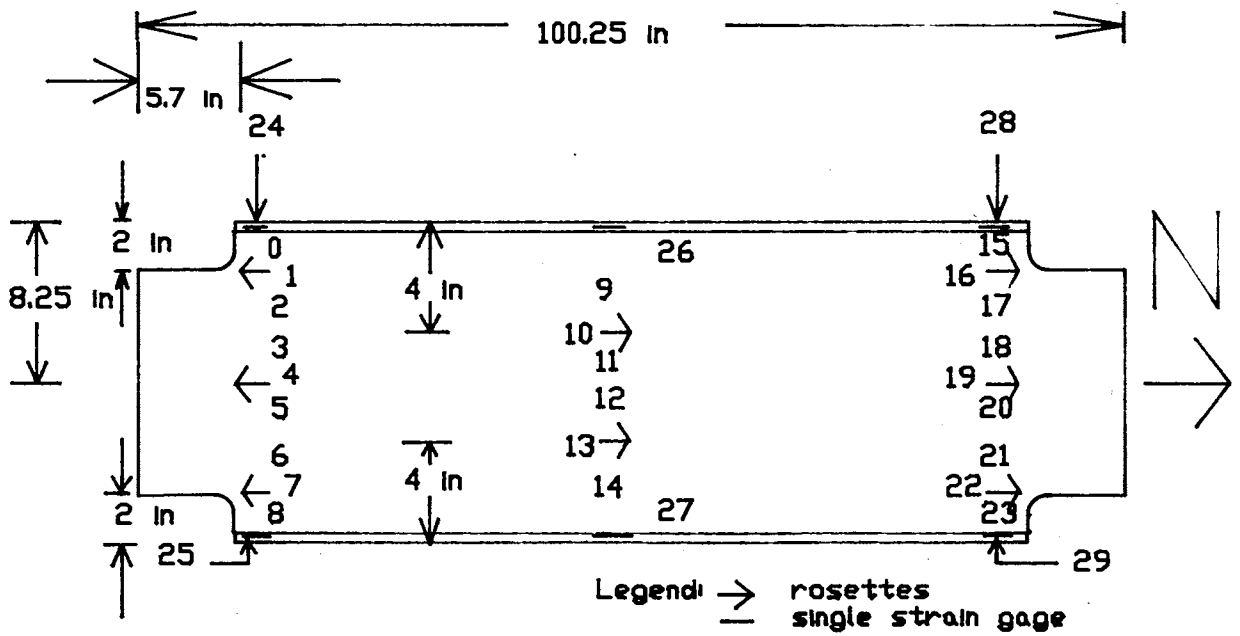

Figure 7. Location of strain gages on laboratory instrumented diaphragm

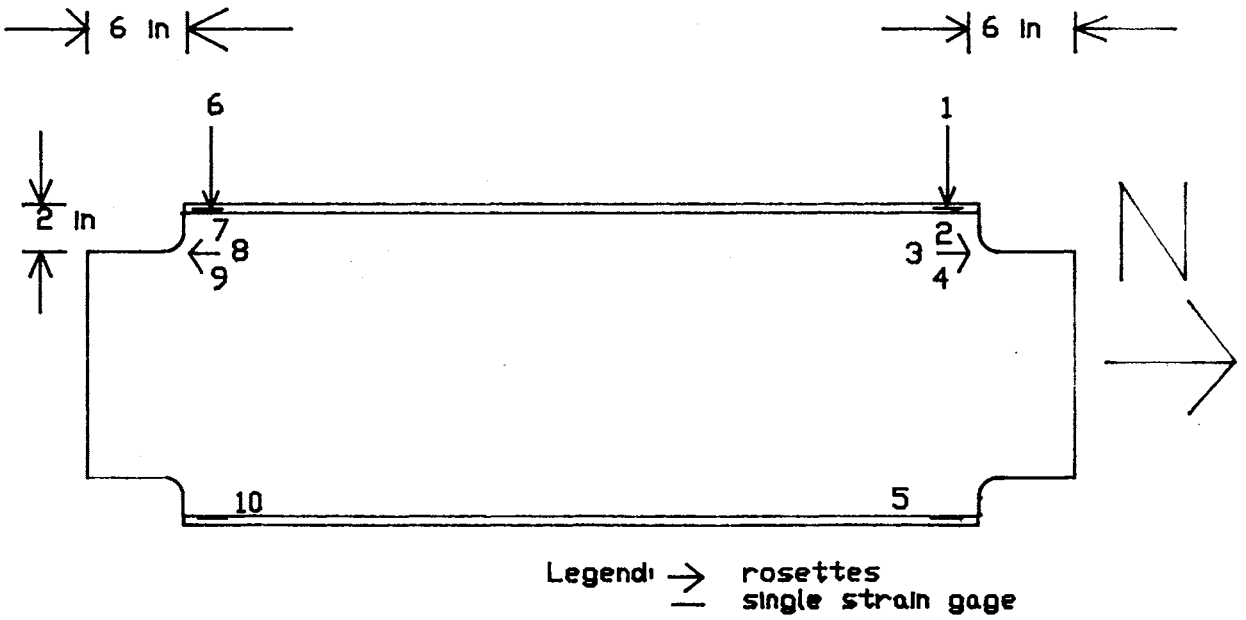

Figure 8. Location of strain gages on field instrumented interior diaphragm

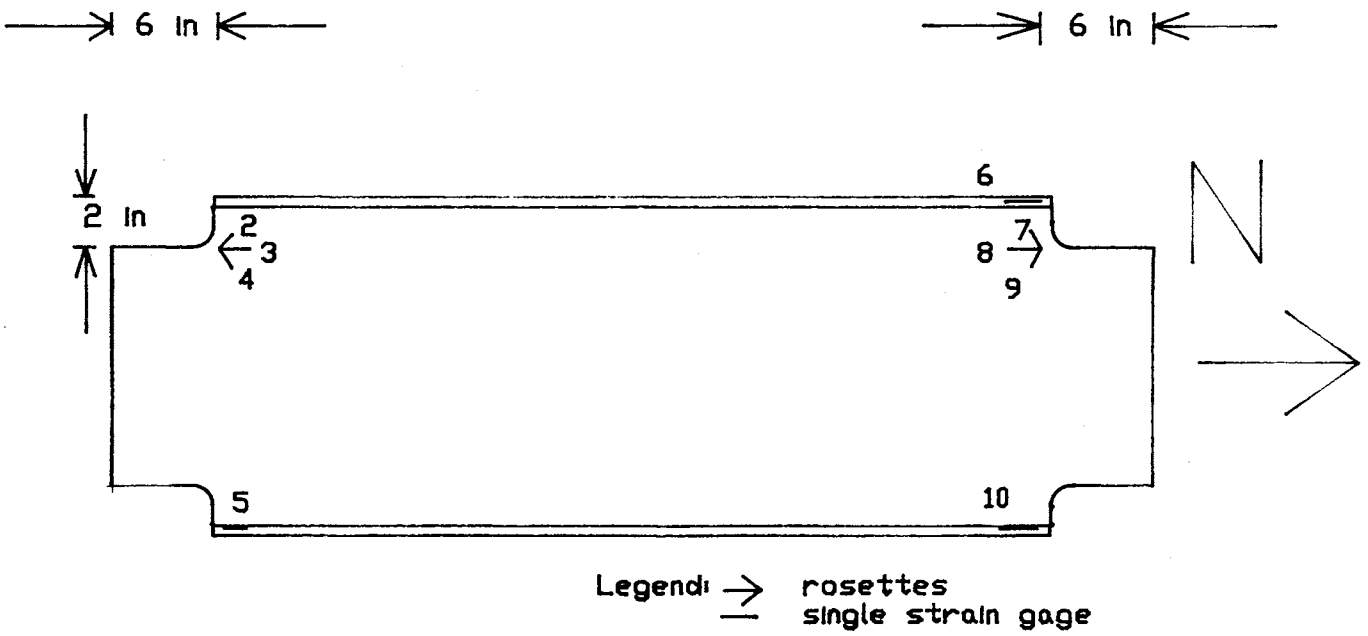

Figure 9. Location of strain gages on field instrumented exterior diaphragm

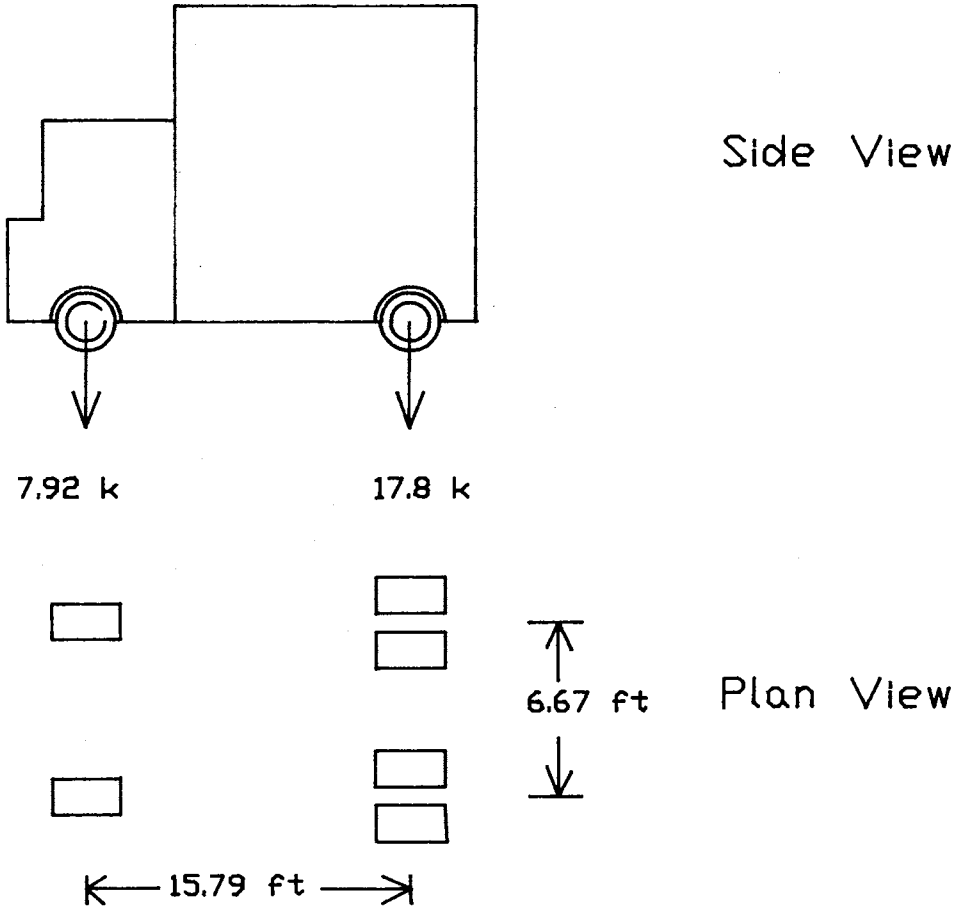

Figure 10. Tank truck used for loading bridge

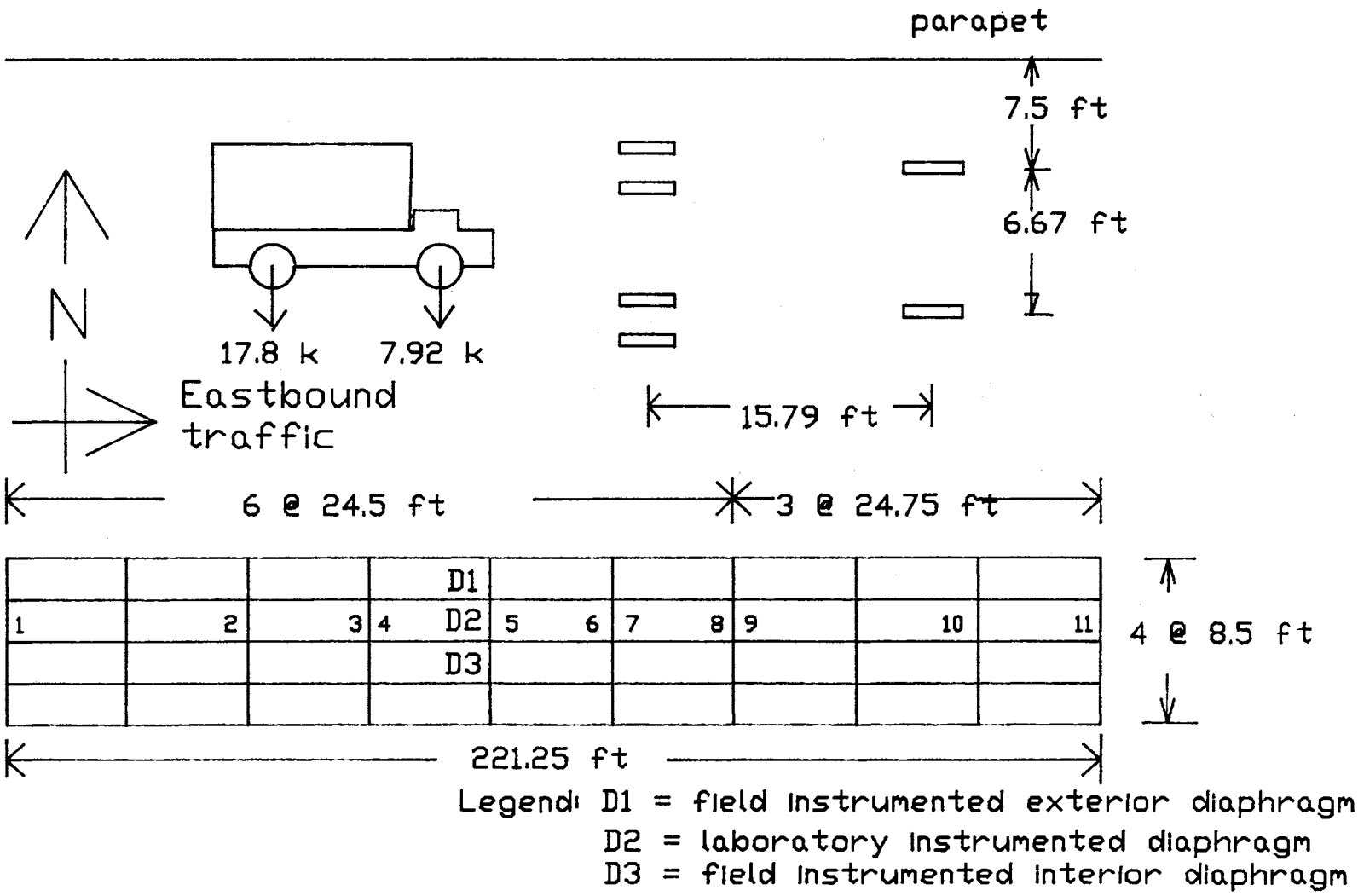

Figure 11. Lane loadings at various positions along first three spans of bridge

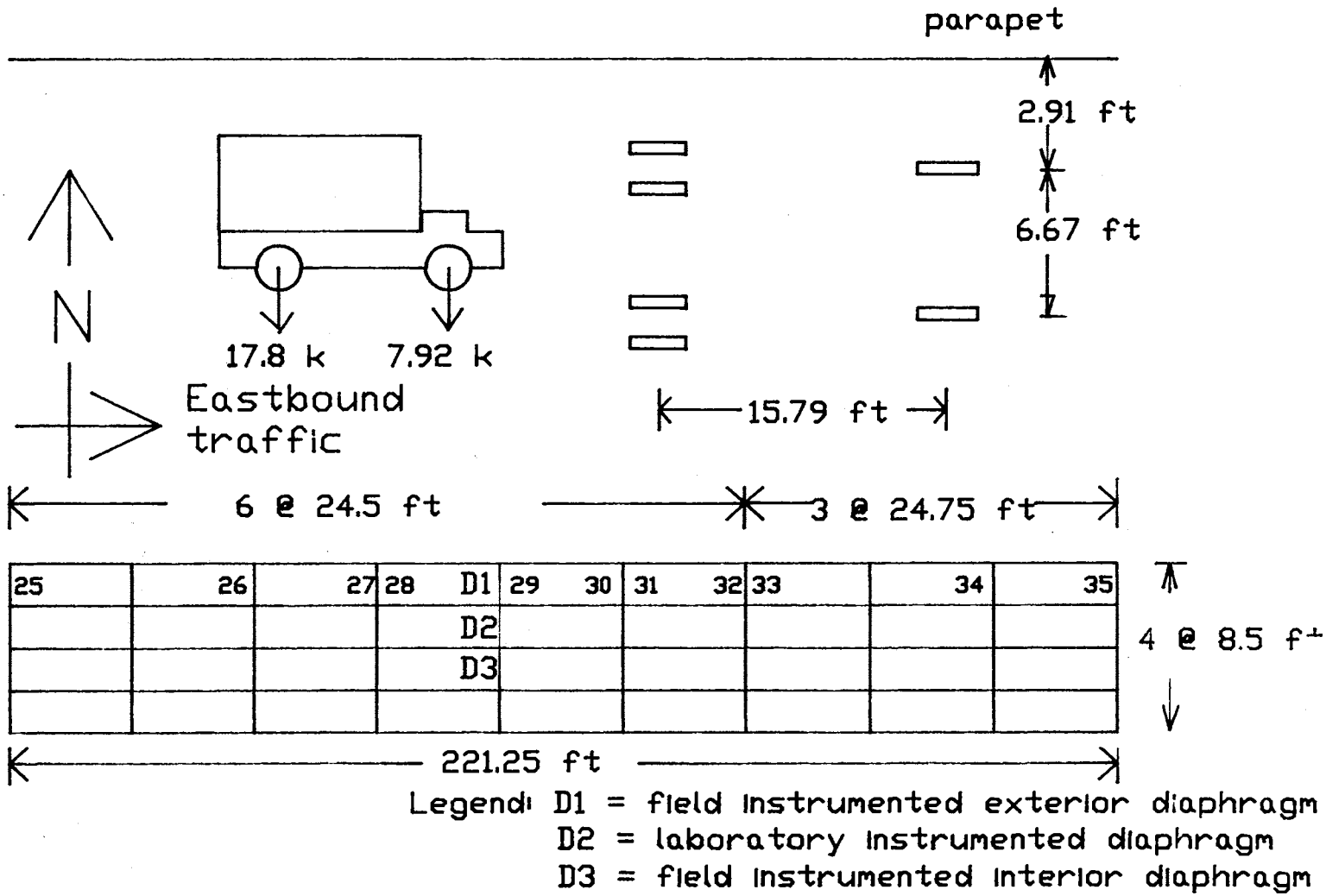

Figure 12. Shoulder loadings at various positions along first three spans of bridge

TABLE I

POSITION OF TRUCK VERSUS DISTANCE ALONG BRIDGE

Position of truck (Lane Loading)	Position of truck (Shoulder Loadings)	Distance of truck along bridge (ft)
1	25	0
2	26	37.75
3	27	58.46
4	28	74.25
5	29	98.75
6	30	111.90
7	31	123.25
8	32	131.96
9	33	147.75
10	34	184.88
11	35	206.96
12	36	222.75
13	37	260.63
14	38	281.96
15	39	297.75
16	40	331.50
17	41	349.46
18	42	365.25
19	43	401.00
20	44	420.96
21	45	436.75
22	46	469.13
23	47	486.71
24	48	502.51

Positions 1-11 and 25-35 are along the first three spans of the seven span bridge. Positions 12-24 and 36-48 are along the fourth to seven spans. The first three spans are continuous and the last four spans are continuous.

shows the position of the truck along the bridge for which measurements were taken. The truck was stopped at each position and strains were recorded when the bridge was clear of all other traffic.

3.2 Analytical Models

This portion of the investigation deals with the development of analytical models of the bridge and the individual diaphragm. These models were built using STRUDL (1,2) on a main-frame computer. The models were built so as to match as closely as possible field conditions. The final model that was adopted for the whole bridge was that of a grid model with full composite action between the slab and the girders and diaphragms (Fig 13). Simple supports were assumed at the piers. The individual diaphragm was modelled using eight-noded quadrilateral isoparametric mesh elements for the web and plane truss members for both the flanges as shown in Figures 14 and 15. All nodes on the left end of the diaphragm are pinned to provide support. Loads applied to the right end of the diaphragm produce the same stress gradient indicated by load tests.

The magnitude of the loads applied to the model diaphragm are ten times those obtained from the analysis of the bridge using the grid model. This was done because when small loads obtained from the grid model were used, a significant error was observed between the nodal stresses for the elements meeting at a node. When small loads were

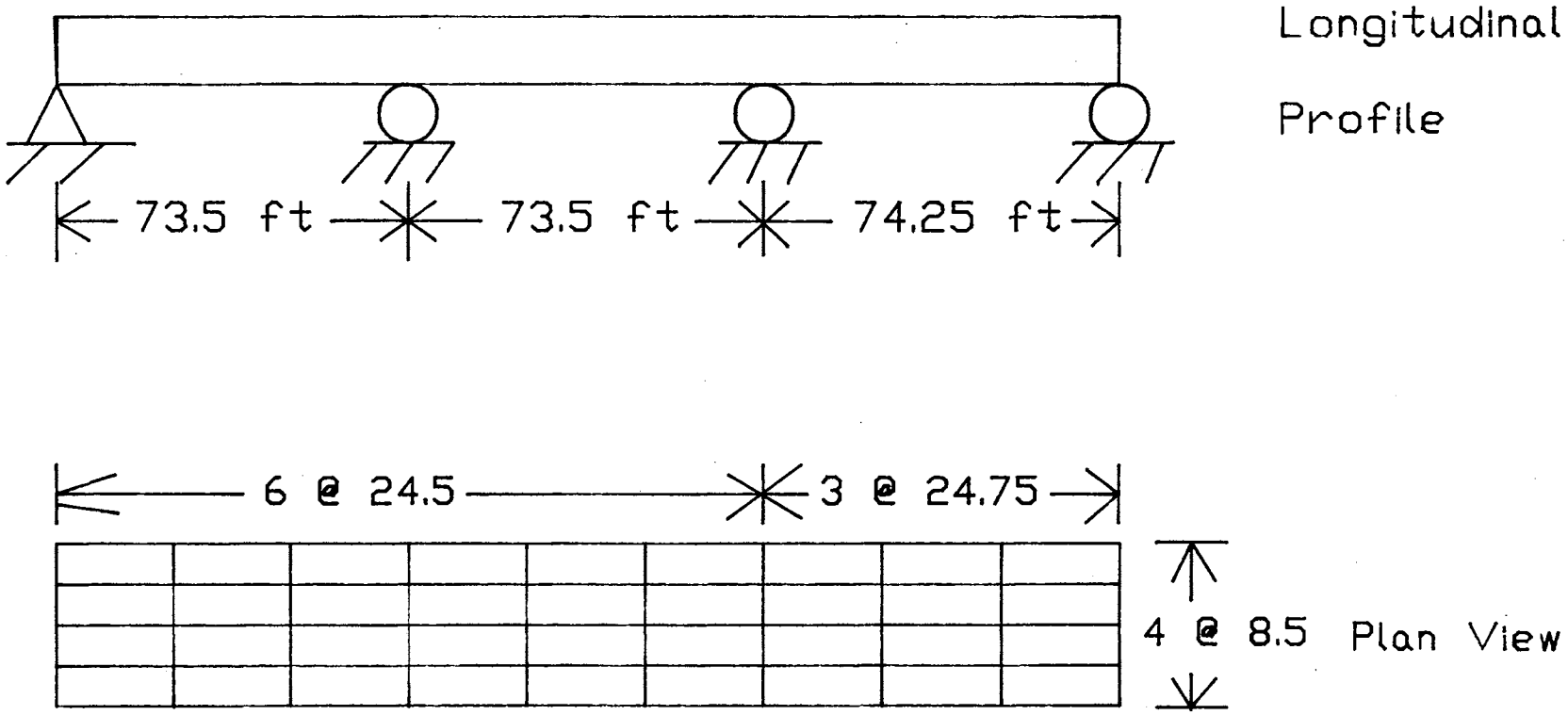

Figure 13. Grid model of first three spans of bridge

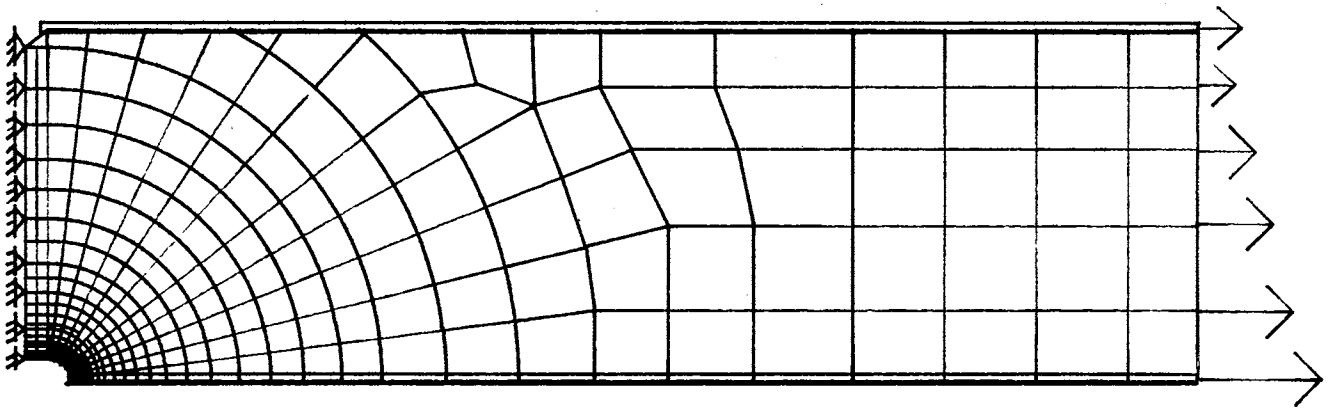

Figure 14. Finite element model for diaphragm with coped bottom flange

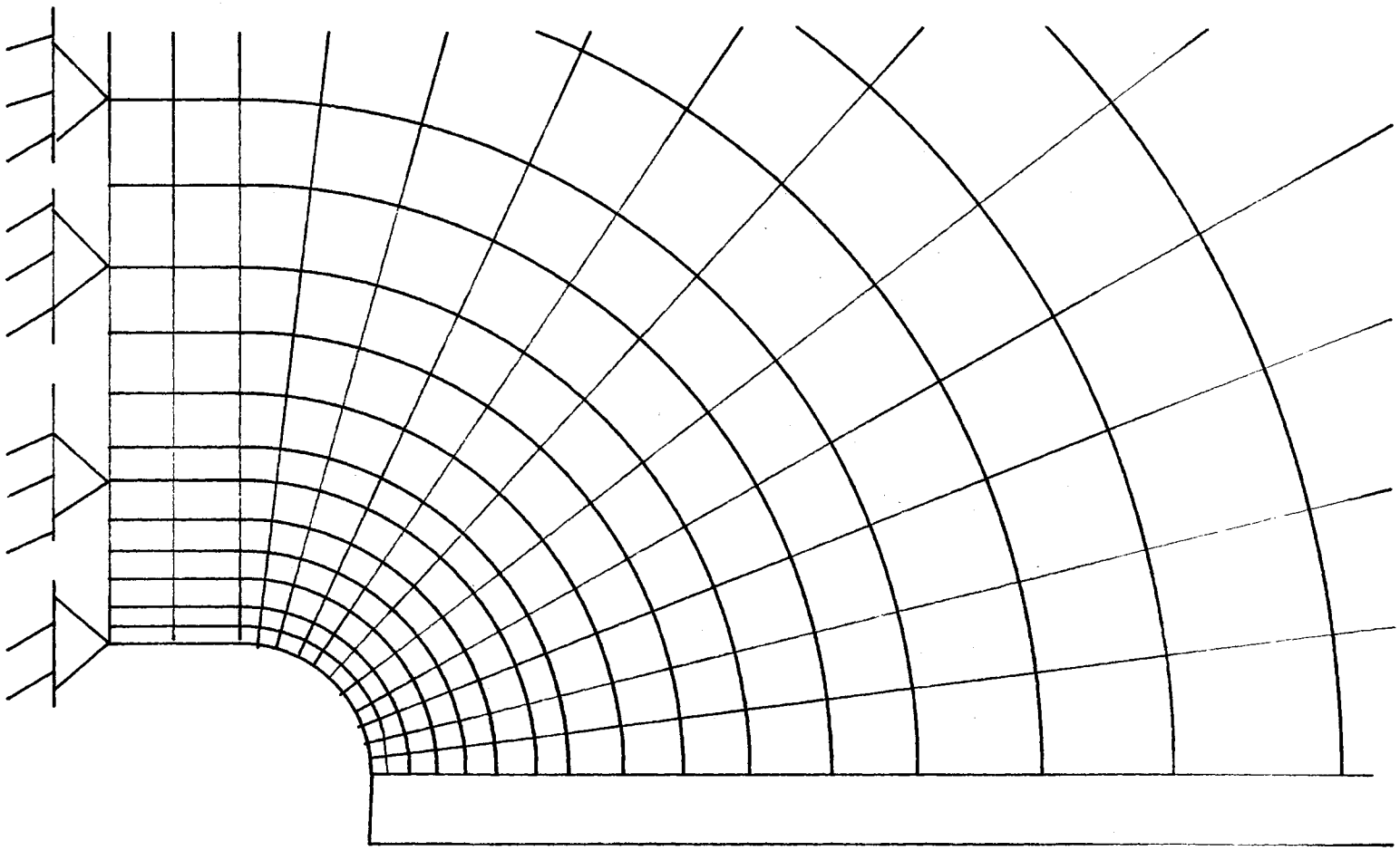

Figure 15. Magnified view of the finite element model near the coped flange

used, the number of significant digits inputted becomes critical which probably contributed to this error. Since the emphasis is to find the stress distribution along the observed crack line of the fractured diaphragm, the loads used were increased by a factor of ten which provided good agreement between the nodal element stresses meeting at a node.

Two other models were analyzed with modified web details. These modifications were made to reduce the stress near the cope. One of the modifications (Fig 16) does not include a cope. The other modification (Fig 17) has a tapered cope. In addition to these modifications, the original model was reanalyzed with the lower half of the supports removed. This is equivalent to taking off the bolts along the bottom half of the diaphragm.

3.3 Laboratory Tests

These tests were carried out to determine the physical and chemical properties of existing diaphragms. The diaphragms removed from the bridge during field work provided the material for the chemical analysis, flat bar tension tests, and Charpy impact fracture tests. Since the design drawings call for ASTM A36 steel, the measured properties are compared with allowable properties of A36 steel.

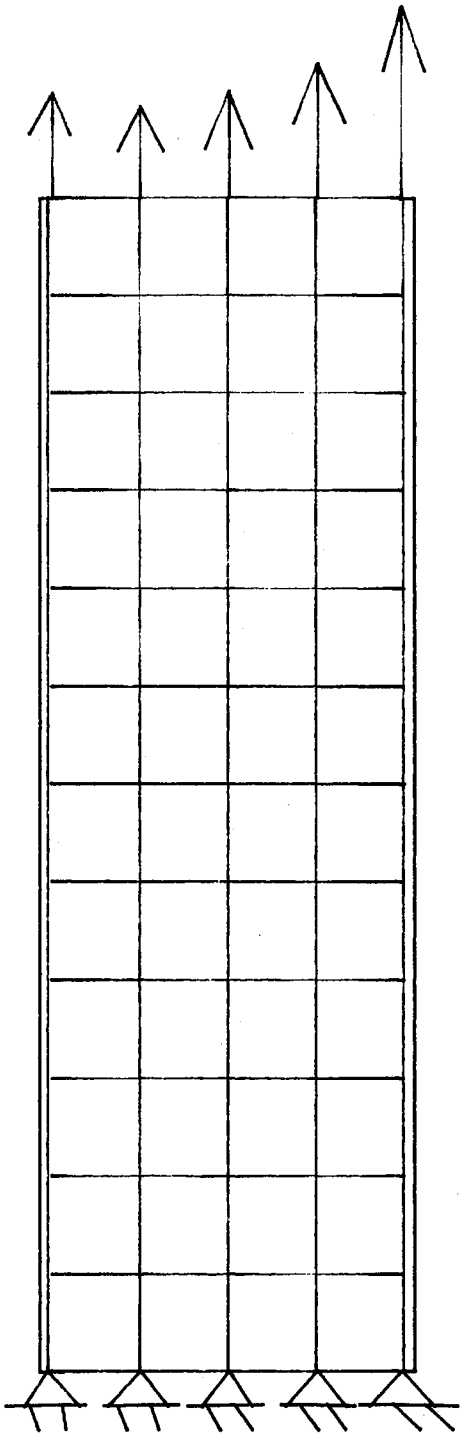

Figure 16. Uncoped diaphragm

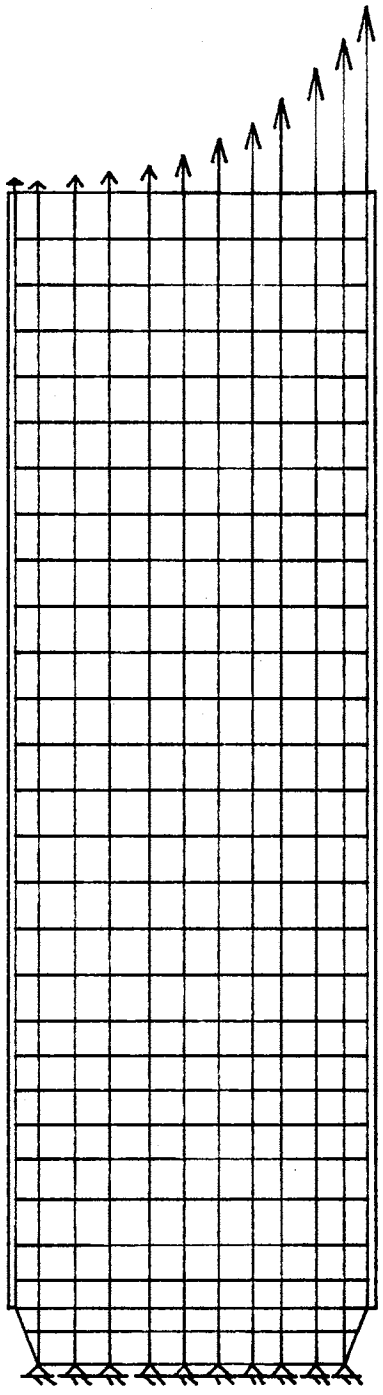

Figure 17. Diaphragm with tapered cope

CHAPTER IV

RESULTS

This research principally involves the analysis of strains measured in diaphragms while the bridge is under a known load. Strains are plotted versus the position of the truck along the bridge and versus diaphragm depth. Measured strains are compared to strains calculated from simple beam theory and from finite element analyses. Chemical composition and mechanical properties of diaphragms are also reported.

4.1 Results from Field Measurements and Grid Model

Plots of strain versus position of truck are provided in Figures 18 and 19. Figure 18 shows the values obtained at gage #22 for the laboratory instrumented diaphragm when the vehicle is located at various positions on the shoulder of the roadway. Figure 19 is a plot for the field instrumented exterior diaphragm at gage #8 for lane loading conditions at different positions along the bridge. The strain data for these plots are tabulated in the appendix.

The strong similarity in graph shapes between the

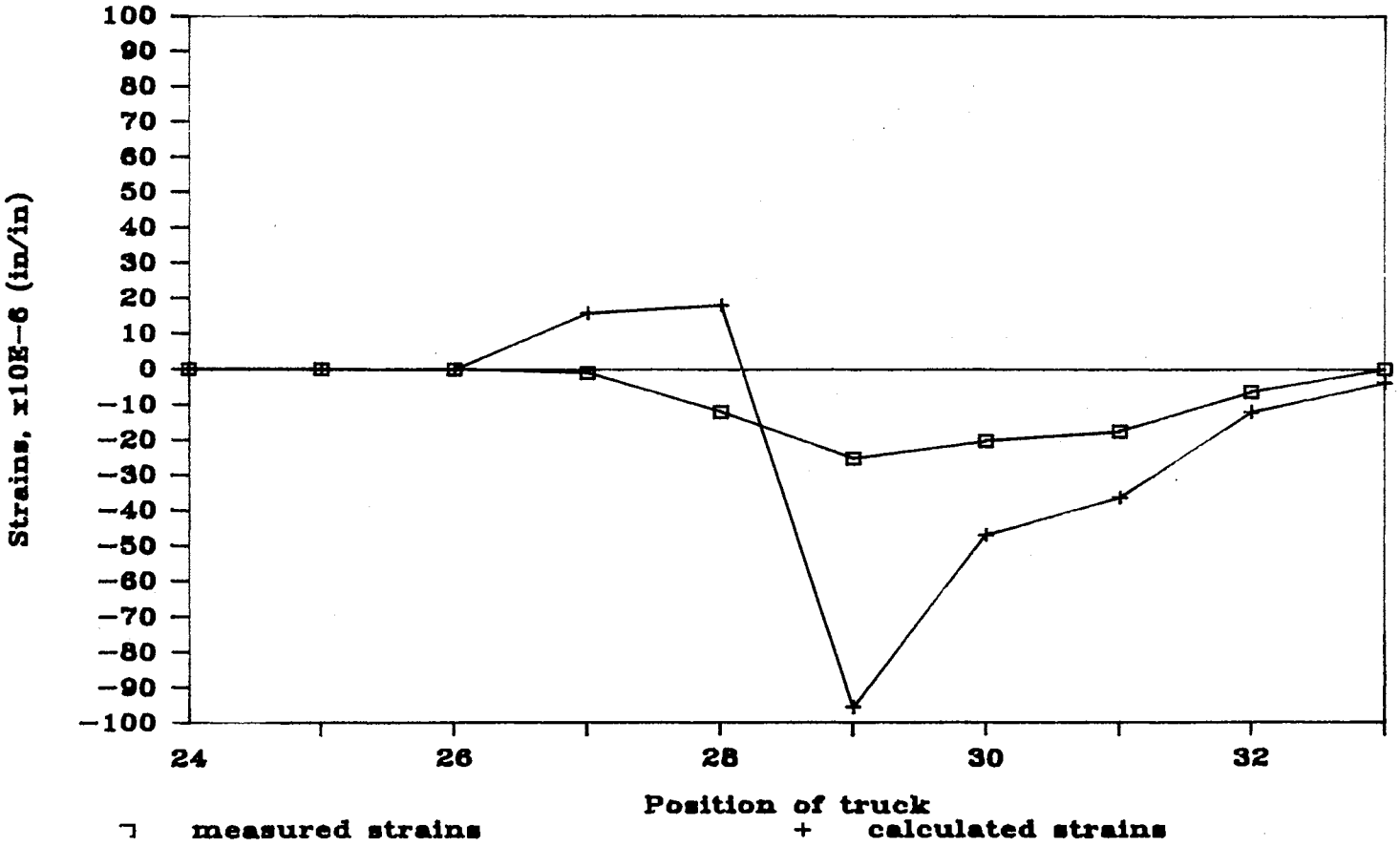

Figure 18. Strains for various shoulder loading positions, laboratory instrumented diaphragm, gage #22

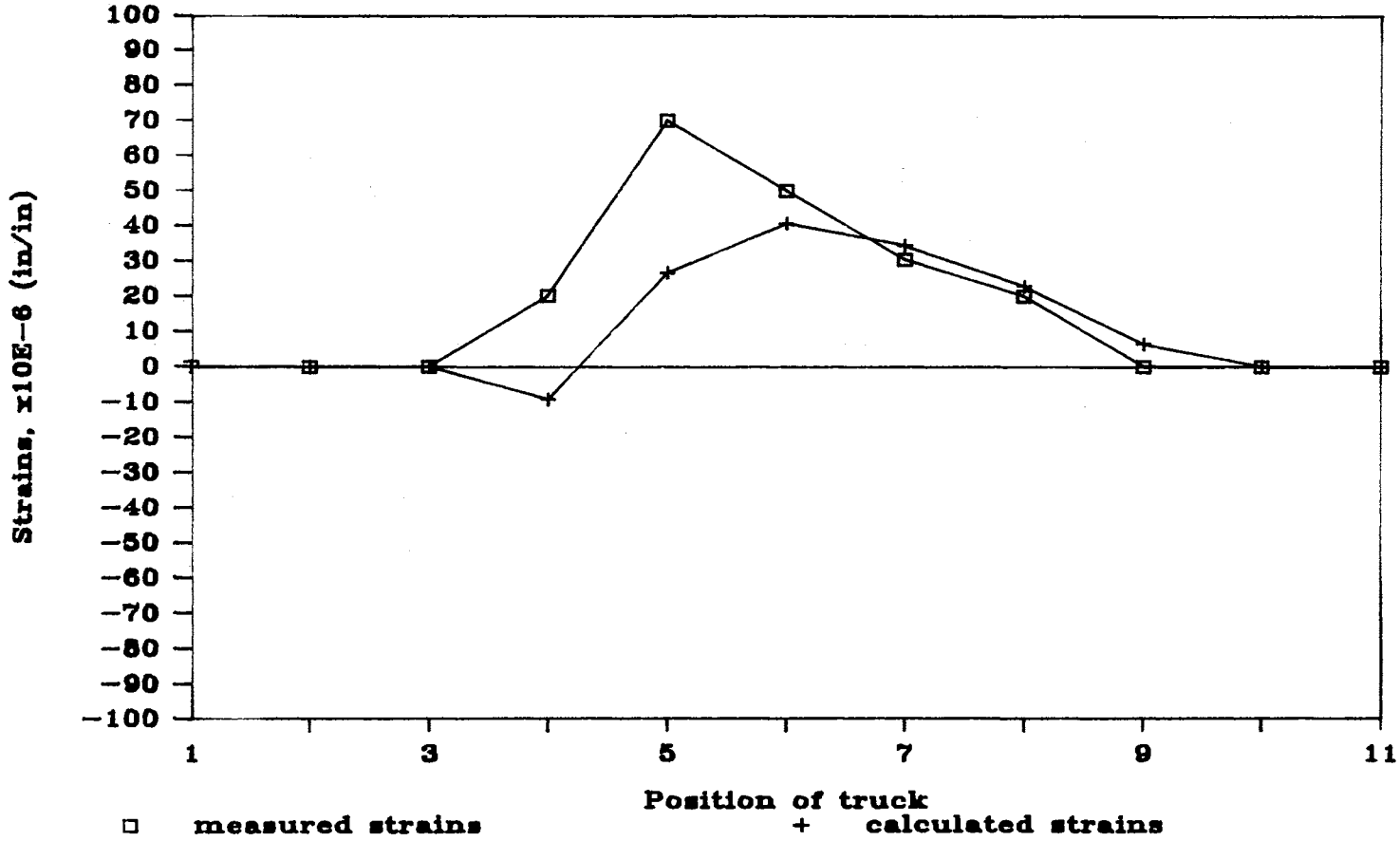

Figure 19. Strains for various lane loading positions, field instrumented exterior diaphragm, gage #8

experimental and theoretical values of strain versus position of the truck indicates that the model used is a good representation of the bridge.

Plot for strain versus time for a moving vehicle is shown in Figure 20. Strains shown are for gage #8 for the field instrumented exterior diaphragm. Plots were made in the field for different vehicle speeds to provide a general picture of the effect of speed on peak strains. The graph shows peak strain increase only a small amount as the speed of the truck increases.

Representative samples of strain versus diaphragm depth results are shown in Figures 21 to 24 for the laboratory instrumented diaphragm. The strain data and gage locations for these plots are tabulated in the appendix. Calculated strains for these plots are based on simple beam theory. Moments used in the calculations are from the grid analysis of the bridge. The load is located at position 5 (lane loading) for Figures 21 and 23 whereas in Figures 22 and 24 the load is located at position 29 (shoulder loading).

Measured and calculated strains along the diaphragm depth do not correlate well, although the variation in strain with depth is similar for some cases. The difference in measured and calculated values might be partially the result of assumptions concerning composite action and simple beam behavior. Differences might also be attributed to the effect of signal noise on the very low strains measured.

Attempts were made to measure the vertical and

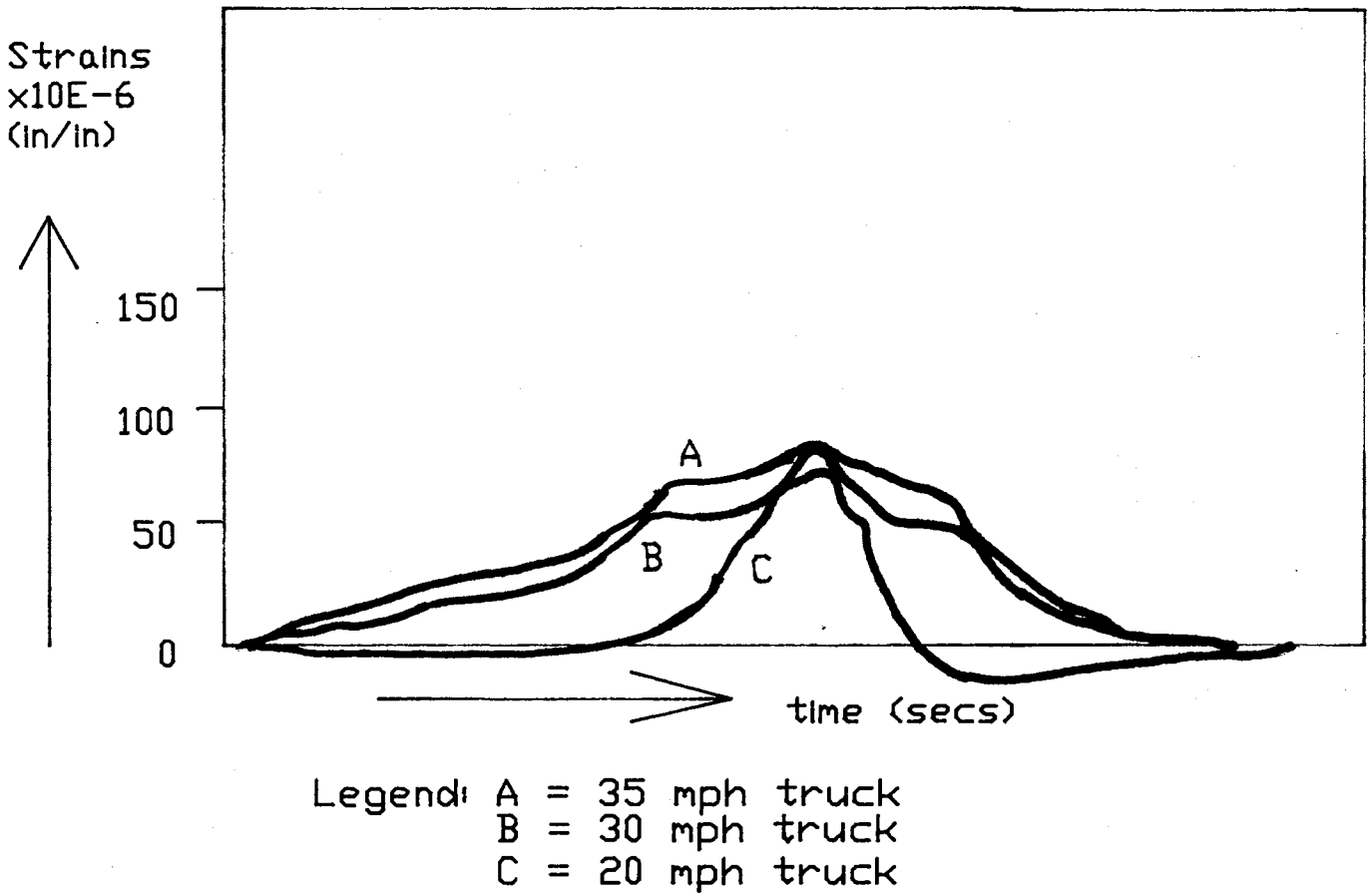

Figure 20. Unscaled plot of strain versus time for different truck speeds

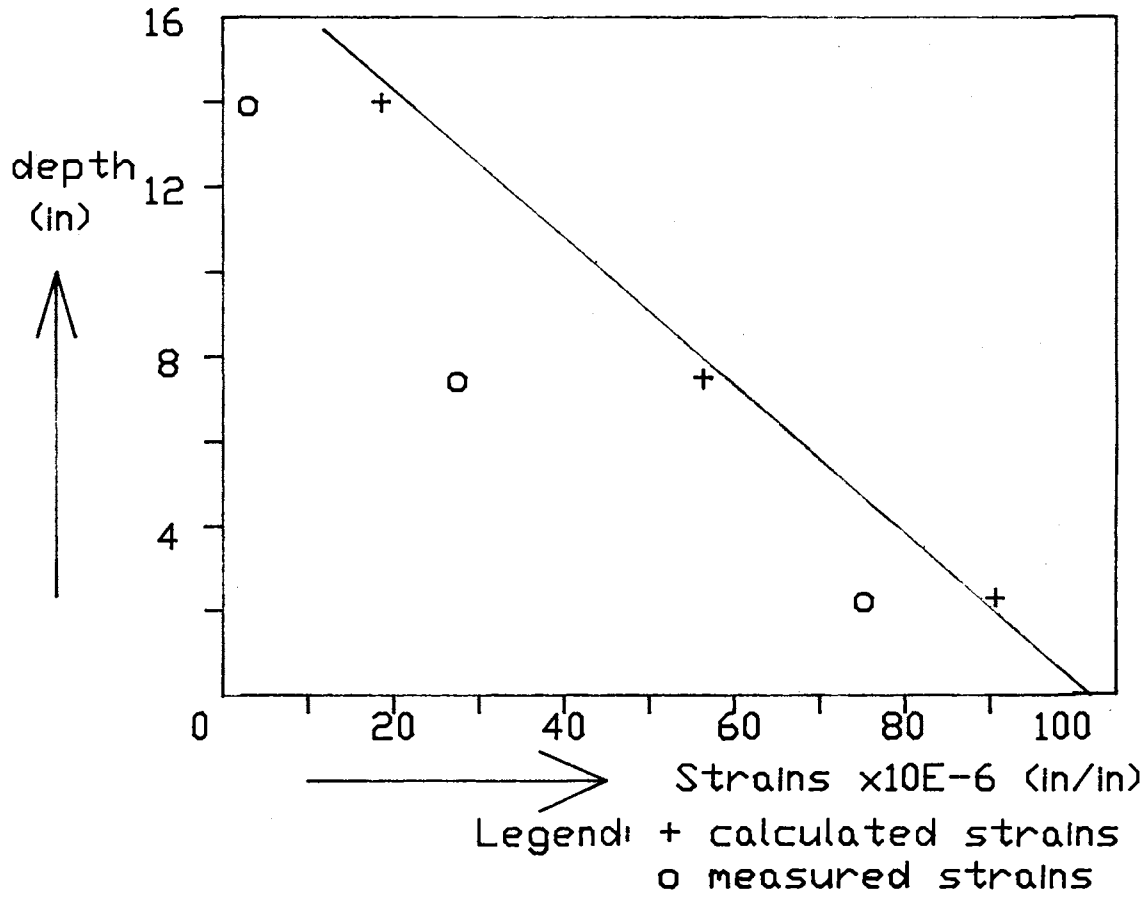

Figure 21. Strain versus depth for laboratory instrumented diaphragm, gages #1,#4,#7, loading at position 5

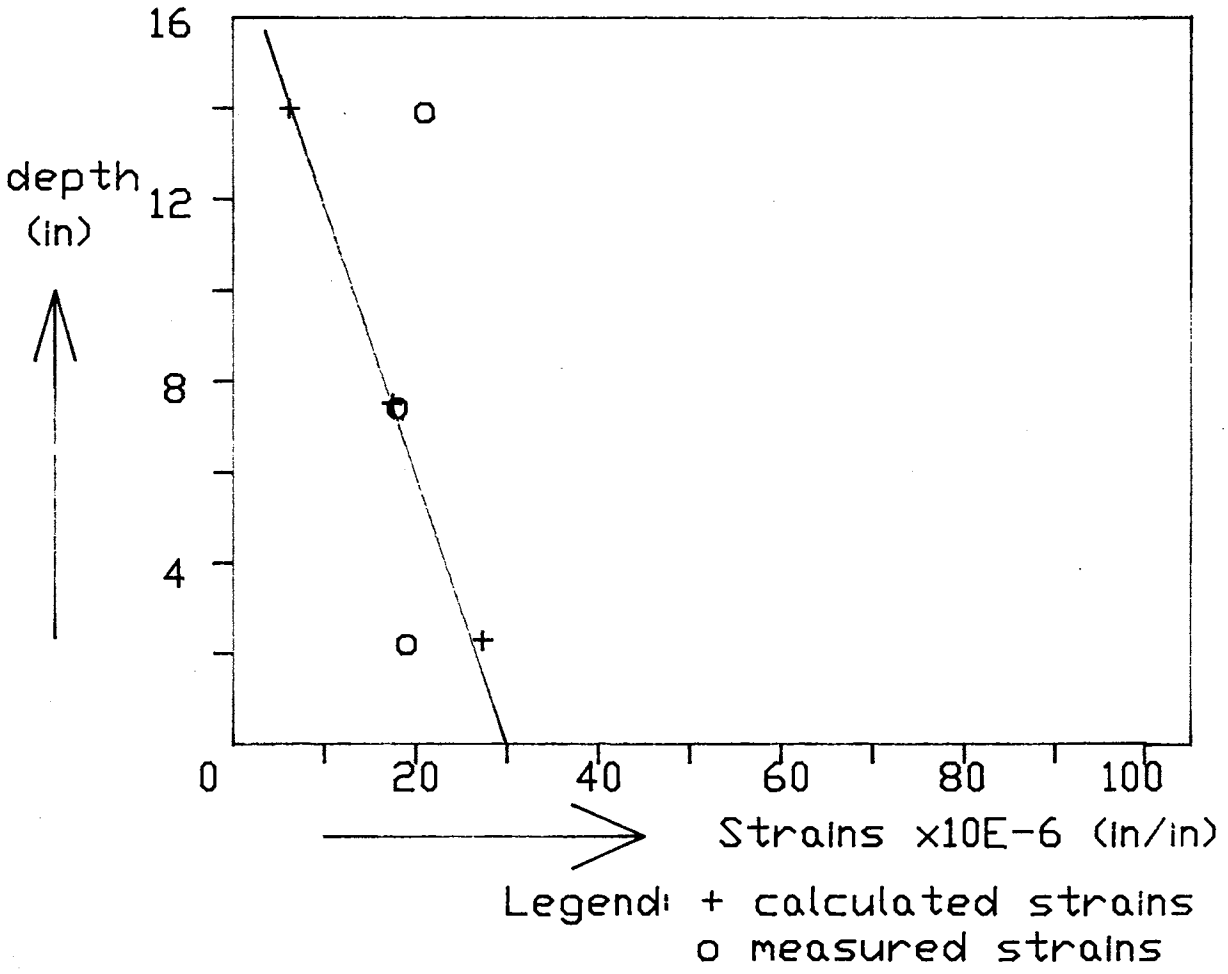

Figure 22. Strain versus depth for laboratory instrumented diaphragm, gages #1,#4,#7, loading at position 29

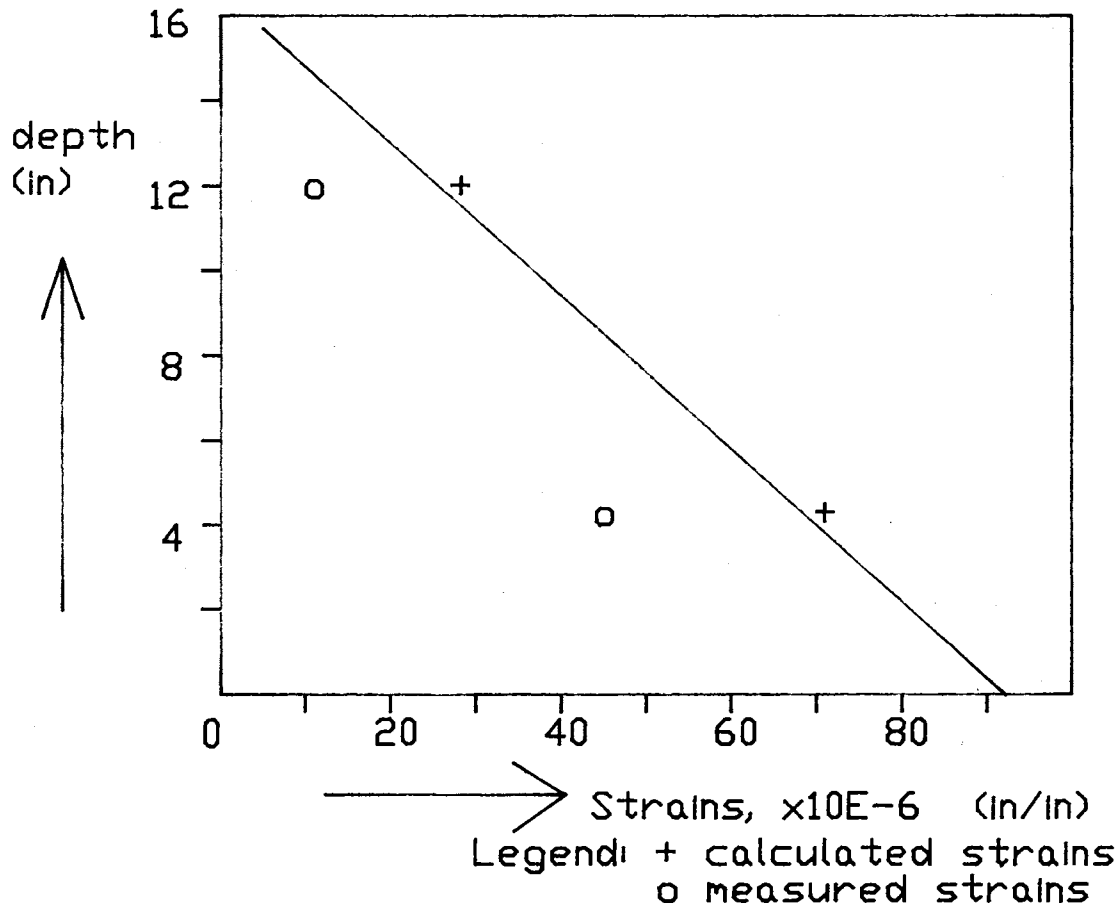

Figure 23. Strain versus depth for laboratory instrumented diaphragm, gages #10,#13, loading at position 5

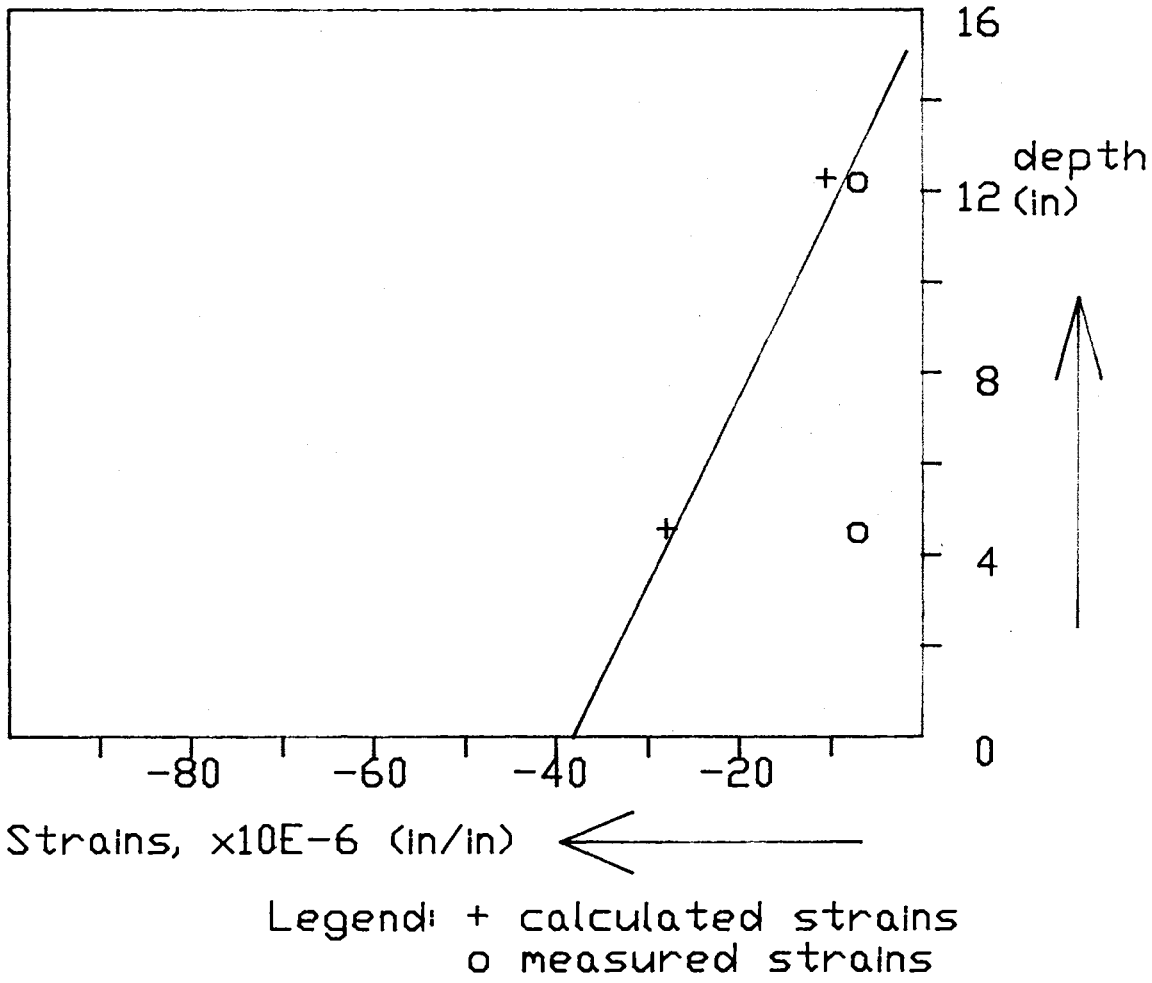

Figure 24. Strain versus depth for laboratory instrumented diaphragm, gages #10,#13, loading at position 29

horizontal displacements of longitudinal members. These attempts proved to be unsuccessful. However, vertical displacements from the grid analysis were plotted (Fig 25) for an interior longitudinal member and the load is located at position 5. The tabulated values are given in the appendix.

4.2 Finite Element Analysis

Stresses calculated along the crack line from the four analytical models are shown in Figure 26. The first three models are shown in Figures 14 to 17. All nodes on the left side of the diaphragms are pin supported. The fourth model is similar to the first except that the lower half of the supports are released. This is equivalent to unbolting the diaphragm from mid depth to the bottom cope. All mesh elements are eight node elements for the web and plane truss members for the flanges.

4.3 Mechanical and Chemical Properties

Results from a chemical analysis of the diaphragm flange material are shown in Table II. The material is within the tolerance limits for ASTM A36 steel.

Mechanical properties of the flange and web of the fractured diaphragm were determined using flat bar tension tests. The web material has a yield strength of 45.33 ksi

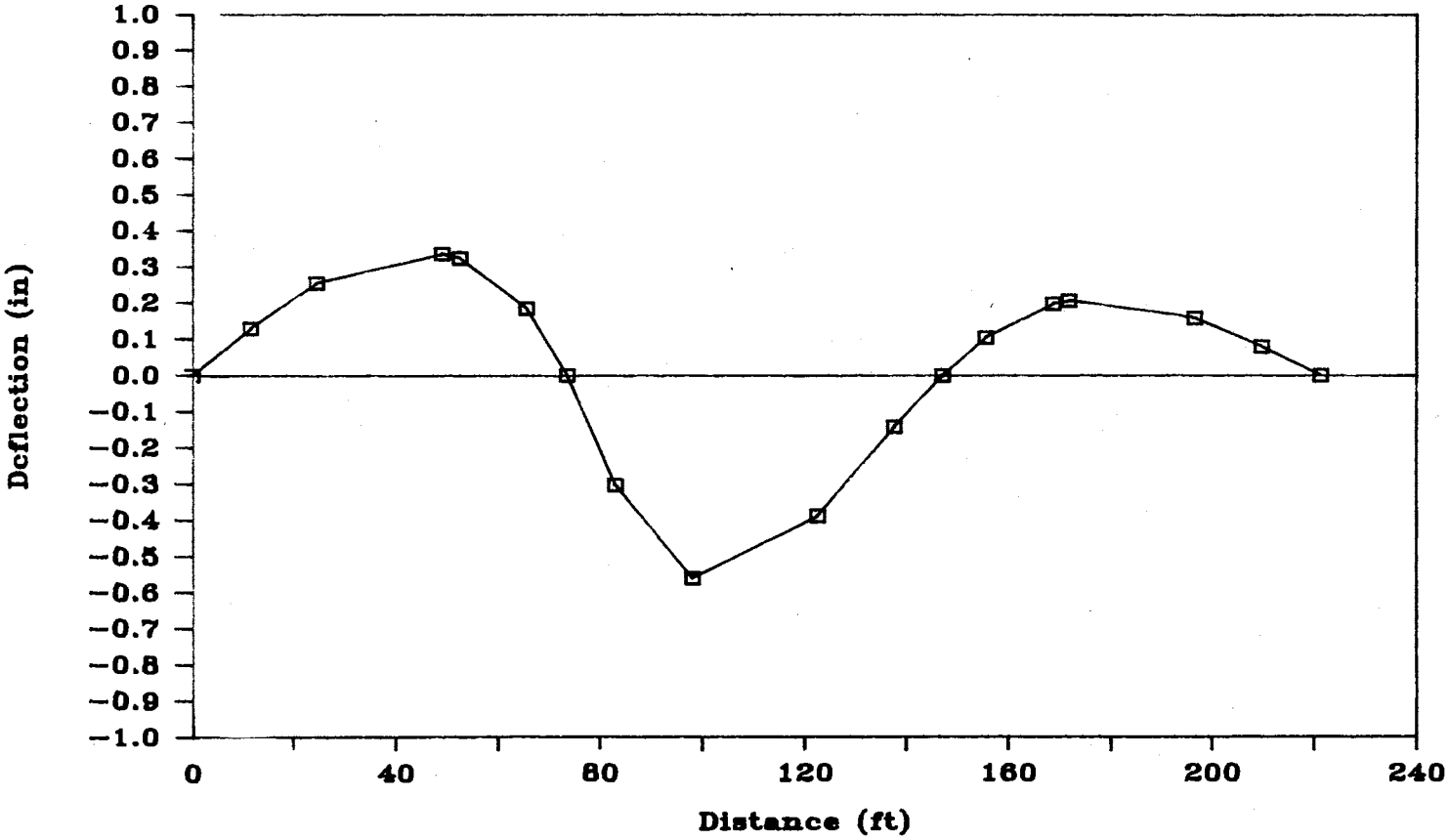

Figure 25. Deflected shape of an interior girder obtained using the grid model, loading at position 5

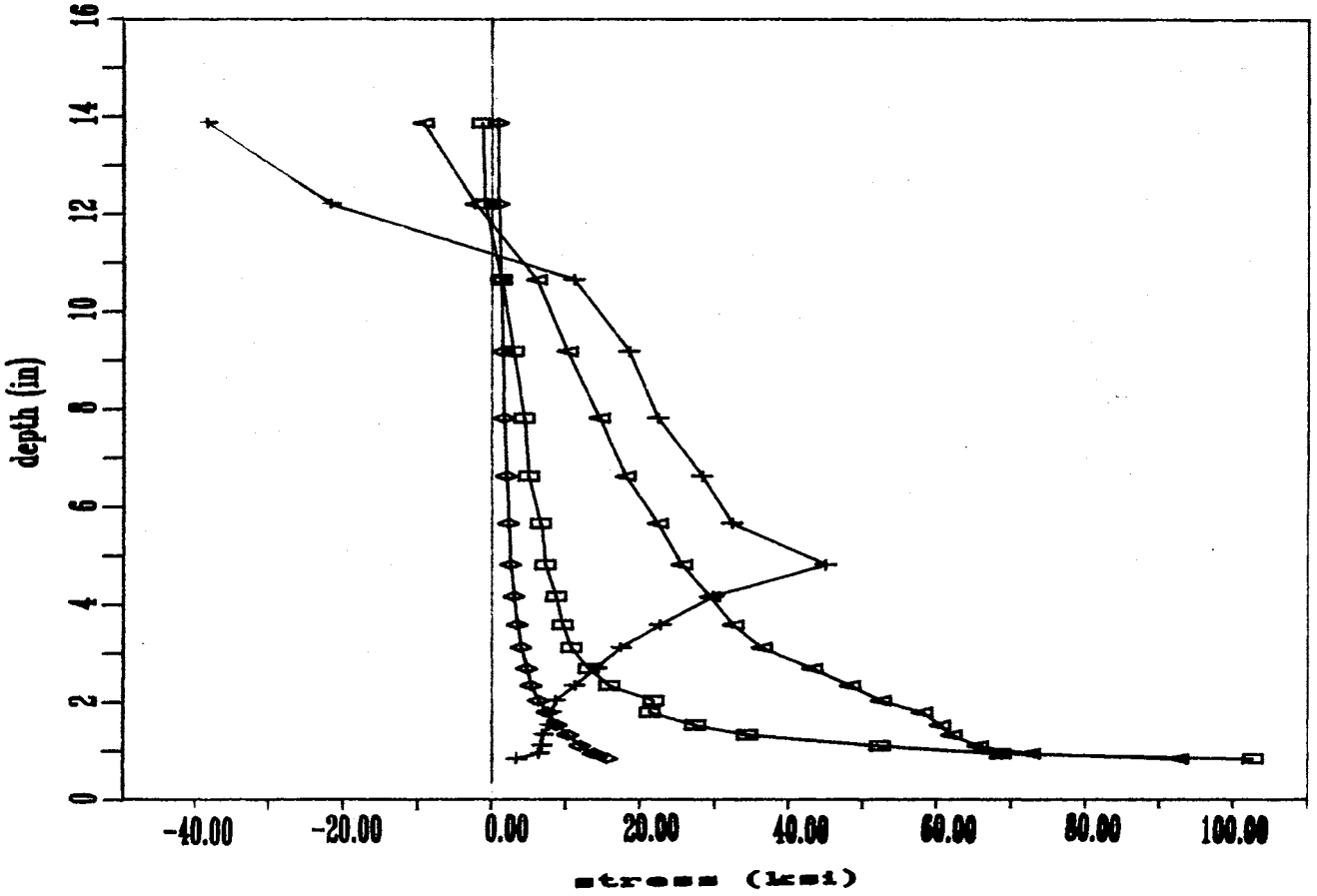

Figure 26. Stress along crack line from finite element models

TABLE II

CHEMICAL PROPERTIES OF WIDE FLANGE

Element	Composition in Percent	ASTM Limits in Percent
Carbon	0.23	0.26 max
Manganese	0.56	- - -
Phosphorous	0.007	0.04 max
Sulfur	0.018	0.05 max
Silicon	0.07	- - -
Nickel	0.02	- - -
Chromium	0.06	- - -
Molybdenum	<0.01	- - -
Copper	0.03	- - -

and a tensile strength of 61.71 ksi, whereas the flange material has a yield strength of 38.8 ksi and a tensile strength of 61.25 ksi. Both the web and flange material have an elongation at fracture of 44% . ASTM specifications require a tensile strength of 58 to 80 ksi, a minimum yield point of 36 ksi, and a minimum elongation of 20% in 8 inches.

The fracture toughness of the diaphragm was assessed using the Charpy V notch impact test. Web tests were done using reduced thickness specimens. The results of these tests are shown in Table III. Charpy data is plotted in Figures 27 and 28. To meet AASHTO specifications, Charpy specimens from the subject bridge must absorb 15 ft-lbs or more at 40 ^{o}F. Tested samples easily satisfy this requirement.

4.4 Discussion of Results

Based on the comparison of the theoretical and experimental strain results obtained, the grid model of the bridge seems to represent the actual conditions quite well. Measured strains are in good agreement with strains calculated on the basis of moments from the grid analysis. Slight deviation in measured strain values as compared to the grid model values is probably due to: 1) stresses in the secondary members being not well defined; 2) the actual bridge structure is more likely to behave in the region between composite and noncomposite action in both

TABLE III

DATA FROM CHARPY IMPACT TESTS

Material Specimens	Temperature (°C)	Energy (ft-lbs)
Flange	-74	1.0
	-21	15.5
	0	15.0
	7	42.0
	12	59.5
	20	57.5
	25	65.0
	96	73.0
Web	-74	1.0
	0	38.0
	25	38.5
	96	40.0

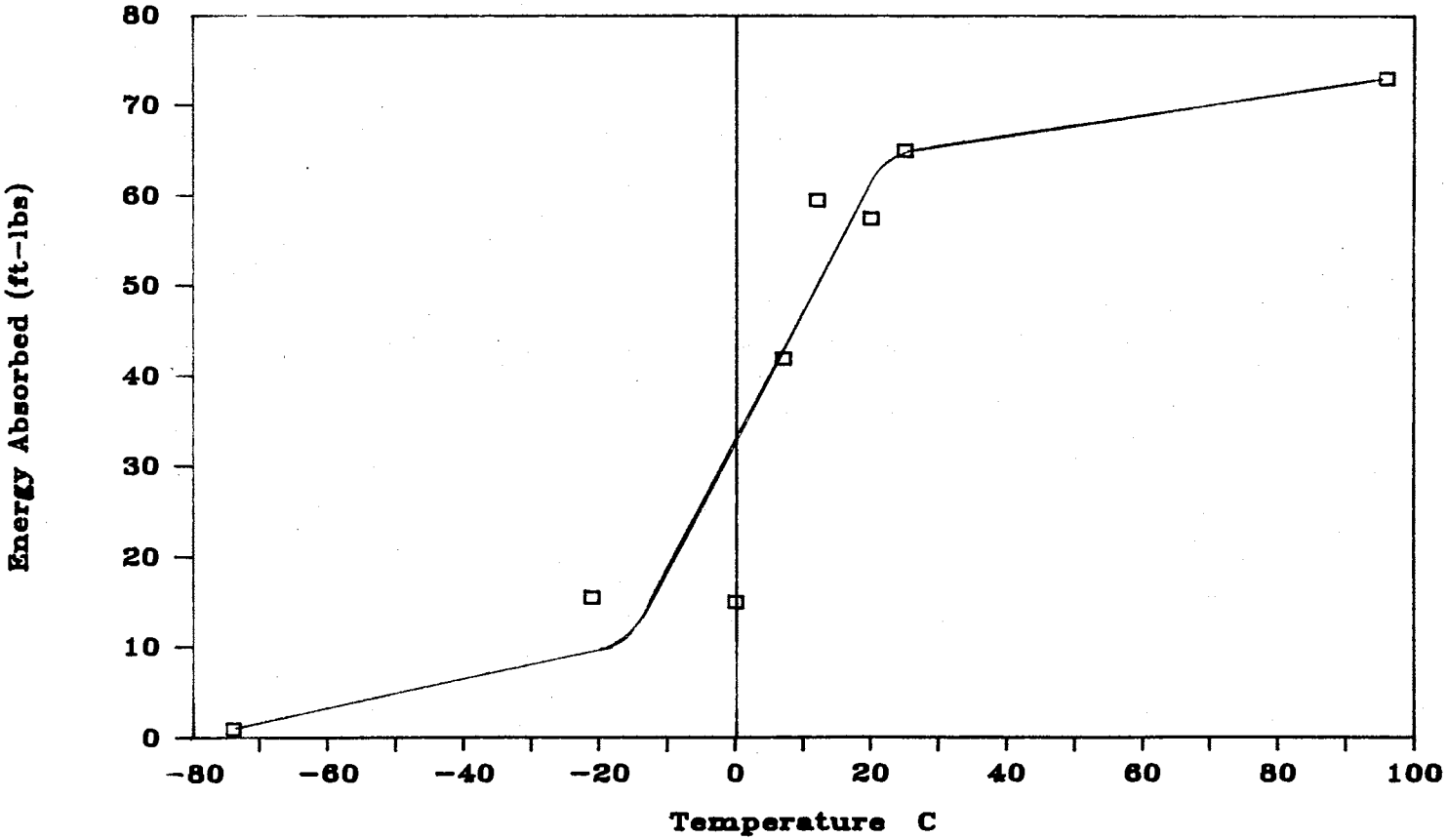

Figure 27. Charpy impact test data for beam flange

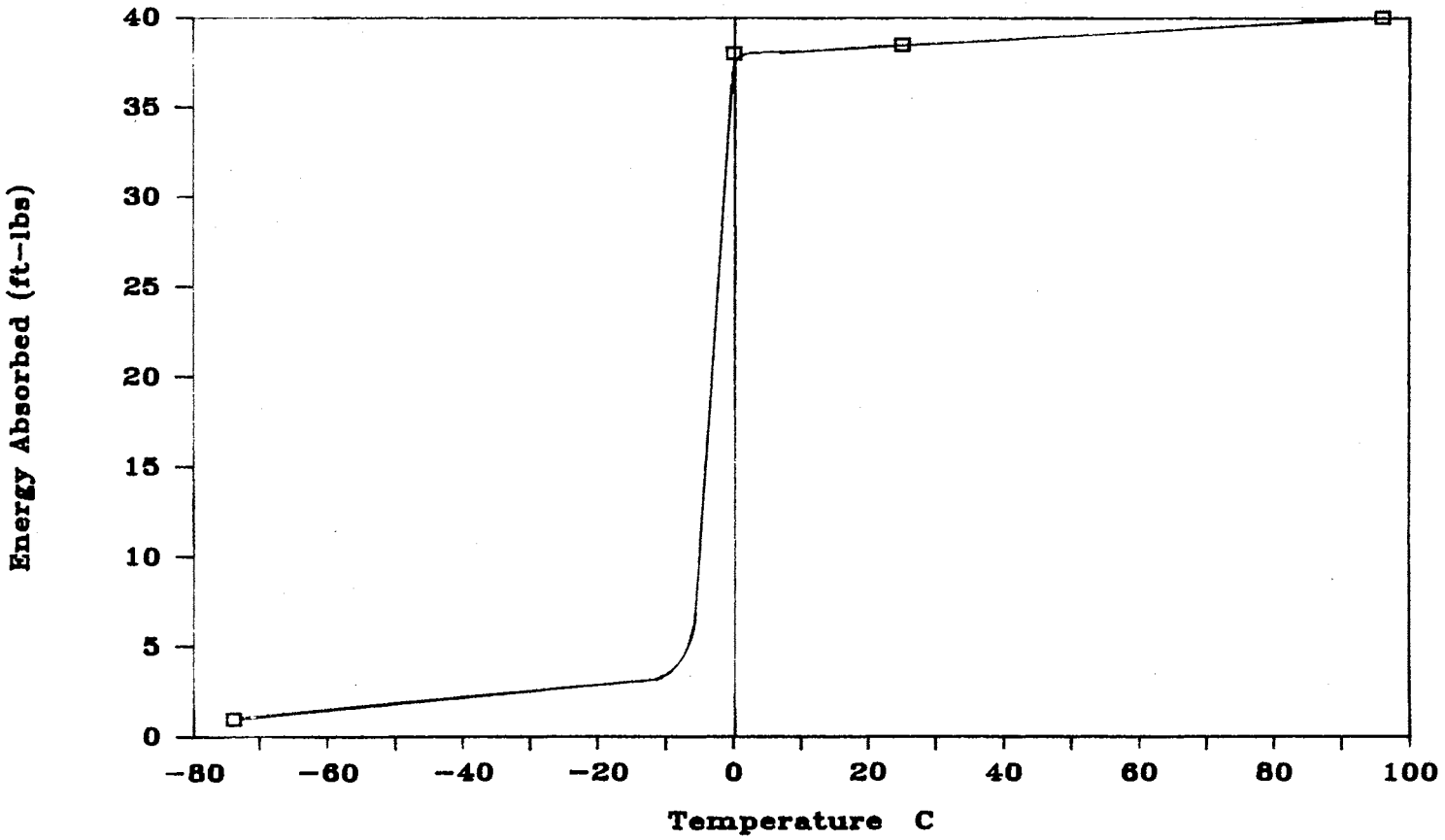

Figure 28. Charpy impact test data for beam web

directions; and 3) simple beam theory was used to calculate stresses.

The finite element model of the diaphragm shows that when low strength details are used (in this case, coping on both top and bottom flanges) a stress concentration will occur at the bottom flange cope which is in tension. The calculated maximum stress in a coped diaphragm is about six times greater than the calculated maximum stress in uncoped diaphragm. Even when the slope of the copes is tapered to a 1:2.5 gradient, the stress concentration factor remains approximately the same as for the original coped diaphragm. When the lower half of the supports of the coped diaphragm are removed, stresses decrease at the cope. The maximum stress occurs at the mid depth of the diaphragm where the last support is found. Furthermore, the magnitude of the stress is reduced by about a factor of three compared to the magnitude of the stress at the coped section when the diaphragms are fully supported.

4.5 Recommendations

Based on the results from the analytical models, the corrective measures that are recommended are: 1) the lower bolts in the diaphragm connections for the uncracked diaphragms should be removed; and 2) cracked diaphragms should be replaced with uncoped diaphragms.

The above recommendations will be tested in the laboratory by controlled fatigue testing. Results from

these tests will be compared to theoretical values.

CHAPTER V

SUMMARY AND CONCLUSIONS

5.1 Summary

When a bridge is loaded by the passage of a vehicle, interior longitudinal members are more heavily loaded than exterior longitudinal members, causing interior girders to deflect more than exterior girders. This differential deflection causes the 'continuous' diaphragms to be bent, resulting in tension along the bottom of the diaphragms. This tension is magnified by the stress concentration at the cope and the residual stress caused by flame cutting. When stress at this point reaches a sufficient magnitude, fatigue crack initiation and propagation will take place.

Evidence that diaphragm bottom flanges are in tension can be seen in the pattern of cracked diaphragms. Evidence of the magnified stress level due to coping is seen in the results of the finite element analysis of the diaphragm. When no coping is done, the stress is about a sixth of the value for the coped diaphragm. These factors lead to the enhancement of growth and propagation of fatigue cracks in coped diaphragms.

5.2 Conclusion

The low strength details of the diaphragms and the loading of the diaphragms due to differential deflections of the longitudinal members are the main factors which lead to fatigue cracks found in diaphragms on this bridge. Under cyclic loading, fatigue cracks will initiate and propagate. The solution to this problem is to relieve the stress concentration found at the bottom cope. This can be achieved by: 1) removing bolts from the lower half of the diaphragms; and 2) replacing cracked diaphragms with uncoped diaphragms.

A SELECTED BIBLIOGRAPHY

1. ICES STRUDL-II, Engineering User's Manual, Vol 1, Cranston : Users Group INC ., 1979

2. ICES STRUDL -II, Engineering User's Manual, Vol 2, MIT, School of Engineering ., 1971

3. Student Manual for Strain Gage Technology, Micro-Measurements Division, MEASUREMENTS GROUP INC., 1978

4. Standard Specifications for Highway Bridges, 13th edition. AASHTO, Washington, D.C., 1983

5. Cudney, G. R., "Stress Histories on Highway Bridges", J. Struct. Div., ASCE, Vol 94, No ST12, Dec 1968

6. Fisher, J. W., Fatigue and Fracture in Steel Bridges, Wiley Interscience, New York, 1984

7. Fisher, J. W., Frank, K.H., Hirt, M.A., and McNamee, B.M., "Effect of Weldments on the Fatigue Strength of Steel Beams", National Cooperative Highway Research Program Report 102, 1970, Transportation Research Board

8. Fisher, J. W., Albretch, P.A., Yen, B.T., Klingerman, D.J., and McNamee, B.M., "Fatigue Strength of Steel Beams With Welded Stiffeners and Attachments", National Cooperative Highway Research Program Report 147, 1974, Transportation Research Board

9. Fisher, J. W., Schiling, C.G., Klippstein, K.H., Barsom, J.M., and Blake, G.T., "Fatigue of Welded Steel Bridge Members Under Variable Amplitude Loadings", National Cooperative Highway Research Program
Report 188, 1978, Transportation Research Board

10. Fisher, J.W., Hausamman, H., Sullivan, M.D., and Pense, A.W., "Detection and Repair of Fatigue Damage in Welded Highway Bridges", National Cooperative Highway Research Program Report 206, 1979, Transportation Research Board

11. Fisher, J. W., Mertz, D.R., and Zhong, A., "Steel Bridge Members Under Variable Amplitude Long Life Fatigue Loading", National Cooperative Highway Research Program Report 267, 1983, Transportation Research Board

12. Fisher, J. W., and Keating P.B., "Fatigue Behavior of Variable Loaded Bridge Details near the Fatigue Limit", Transportation Research Record 1118

13. Fisher, J. W., Bridge Fatigue Guide -Design and Details, American Institute of Steel Construction, 1977

14. Fisher, J. W., Yen, B.T., and Wagner, D.C., "Review of Field Measurements for Distortion Induced Fatigue Cracking in Steel Bridges", Transportation Research Record 1118

15. Fisher, J. W and Pense, Alan., "Experience with Use of Heavy W shapes in tension", Proceedings National Engineering Conference & Conference of Operating Personnel, AISC, April 1987, New Orleans Pg 18-1 to 18-47

16. Ghosn, Michael., Moses, Fred., and Gobieski, John., "Evaluation of Steel Bridges Using In Service Testing", Transportation Research Board Record 1072

17. Hays, Clifford O. Jr., Sessions, Larry M., and Berry, Alan J., "Further Studies on Lateral Load Distribution using Finite Element Method", Transportation Research Record 1072

18. Heins, C. P., and Galambos, C. F., "Bridge Fatigue due to Daily Traffic", Transportation Research Board Record 207

19. Imbsen, Roy A., and Nutt.Richard V., "Wheel Load Distribution on Beam and Slab Highway Bridges", National Cooperative Highway Research Program Project 12-26, Transportation Research Board

20. Kostem, Celal N., and DeCastro, Ernesto S., "Effects of Diaphragms on Lateral Load Distribution in Beam Slab Bridges", Transportation Research Board Record 645

21. Kulicki, John M., Marquiss, Steven W., and DeStefano, Ralph J., "Finite Element Analysis of Cracked Diaphragm Welds on the Ohio Bridge at Wheeling, West Virginia", Transportation Research Record 1044

22. Moses, F. M., Goble, G., and Pavia, A., "Truck Loading Model for Bridge Fatigue", Specialty Conference on Metal Bridges, ASCE, Nov 1974

23. Smith, D. W., "Bridge Failures", Proceedings Institution of Civil Engineers, Part 1, Aug 1976, Pg 367-382

24. Sanders, W. W., "Distribution of Wheel Loads on Highway Bridges", National Cooperative Highway Research Program Report 83, 1970, Transportation Research Board

25. Walker, William H., "Lateral Load Distribution on Multi-girder Bridges", American Iron and Steel Institute Project 332, Pg 34-1 to 34-17

APPENDIX

ADDITIONAL TABLES AND GRAPHS

TABLE IV

STRAIN VERSUS DEPTH OF DIAPHRAGM

Loading Condition	Gage No.	Measured Strains $(10^{-6}$ in/in)	Calculated Strains $(10^{-6}$ in/in)
Lane Loading @ Position 5	1	2	18
	4	26	55
	7	74	90
	10	10	27
	13	44	70
Shoulder Loading @ Position 29	1	20	5
	4	17	16
	7	18	26
	10	-8	-12
	13	-8	-29

TABLE V

STRAIN VERSUS POSITIONS OF TRUCK FOR GAGE #22,
LABORATORY INSTRUMENTED DIAPHRAGM

Loading Condition	Position No.	Measured Strains $(10^{-6}$ in/in)	Calculated Strains $(10^{-6}$ in/in)
Shoulder Loading	24	0	0
	25	0	0
	26	0	0
	27	-1	16
	28	-12	18
	29	-25	-96
	30	-20	-47
	31	-17	-36
	32	-6	-12
	33	0	-4

TABLE VI

STRAIN VERSUS POSITIONS OF TRUCK FOR FIELD INSTRUMENTED EXTERIOR DIAPHRAGM, GAGE #8

Loading Condition	Position No.	Measured Strains $(10^{-6}$ in/in)	Calculated Strains $(10^{-6}$ in/in)
Lane Loading	1	0	0
	2	0	0
	3	0	0
	4	20	-9
	5	70	27
	6	50	41
	7	30	34
	8	20	23
	9	0	6
	10	0	0
	11	0	0

TABLE VII

CALCULATED DISPLACEMENT VERSUS DISTANCE ALONG BRIDGE FOR THE INTERIOR GIRDER

Distance along bridge (ft)	Displacement (in)
0	0
11.5	0.13
24.5	0.26
49.0	0.34
52.5	0.33
65.5	0.19
73.5	0
83.0	-0.30
98.0	-0.56
122.5	-0.39
137.5	-0.14
147.0	0
155.5	0.11
168.75	0.20
171.75	0.21
196.5	0.16
209.75	0.08
221.25	0

TABLE VIII

CALCULATED STRESS VERSUS DISTANCE FROM BOTTOM COPE

Dist (in)	Isop. Quad elem. with cope. Pin supported. (ksi)	Isop. Quad elem. with cope. Upper half pin sopported. (ksi)	Rect. Isop. elem. with no cope. Pin supported. (ksi)	Rect. Isop. elem. with tapered gradient. Pin supported. (ksi)
0.8453	102.5	3.4	15.5	92.5
0.9465	68.6	6.4	13.7	72.5
1.1061	52.3	6.7	11.9	65.5
1.3274	34.4	6.9	10.3	62.0
1.5240	27.4	7.7	8.8	60.5
1.7857	21.3	8.2	7.5	58.0
2.0240	21.8	8.7	6.4	52.5
2.3333	15.9	11.3	5.4	48.3
2.6846	13.1	14.1	4.7	43.2
3.1161	10.8	17.4	4.0	36.4
3.5833	9.6	22.7	3.5	32.5
4.1667	8.7	29.8	3.0	29.4
4.8214	7.3	45.0	2.6	25.6
5.6700	6.6	32.3	2.3	22.4
6.6039	5.0	28.3	2.0	18.0
7.8150	4.4	22.4	1.7	14.5

TABLE VIII (Continued)

Dist (in)	Isop. Quad elem. with cope. Pin supported. (ksi)	Isop. Quad elem. with cope. Upper half pin supported. (ksi)	Rect. Isop. elem. with no cope. Pin supported. (ksi)	Rect. Isop. elem. with tapered gradient Pin supported. (ksi)
9.1786	2.9	18.5	1.5	10.2
10.6548	1.3	11.1	1.2	6.1
12.2084	-0.9	-21.7	1.0	-2.2
13.8632	-1.32	-38.3	0.9	-9.2

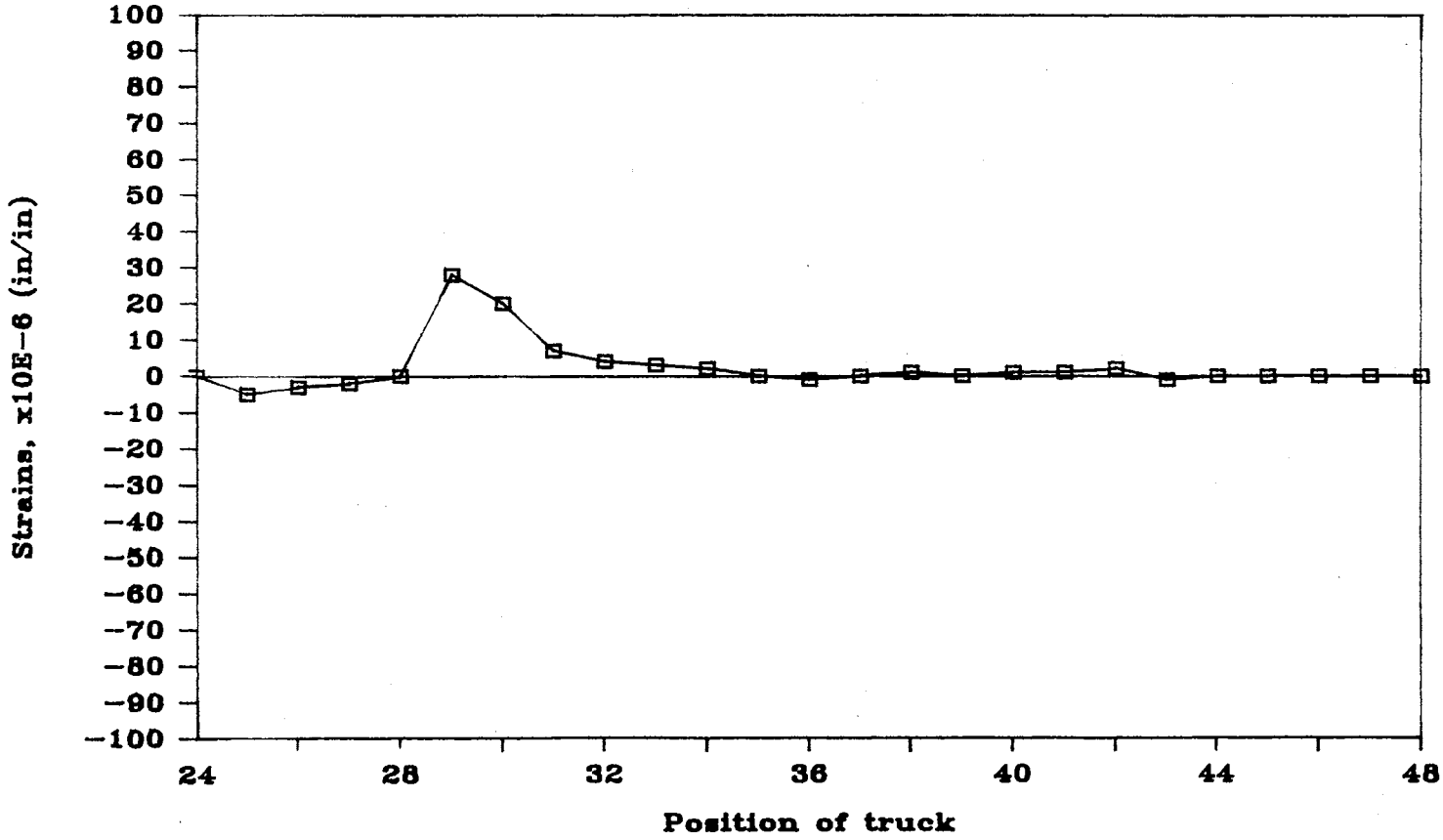

Figure 29. Strains for various shoulder loading positions, laboratory instrumented diaphragm, gage #0

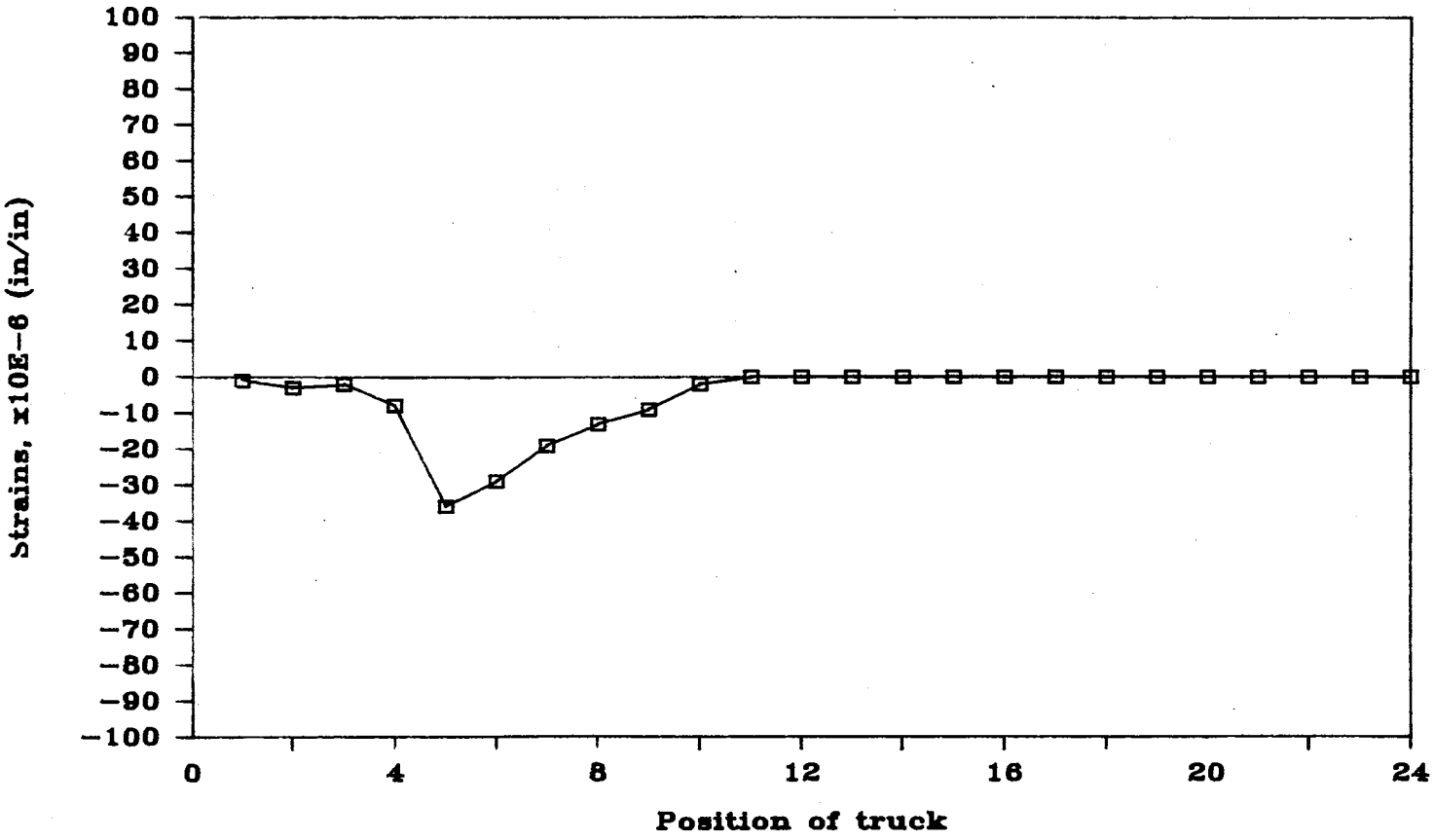

Figure 30. Strains for various lane loading positions, field instrumented diaphragm, gage #2

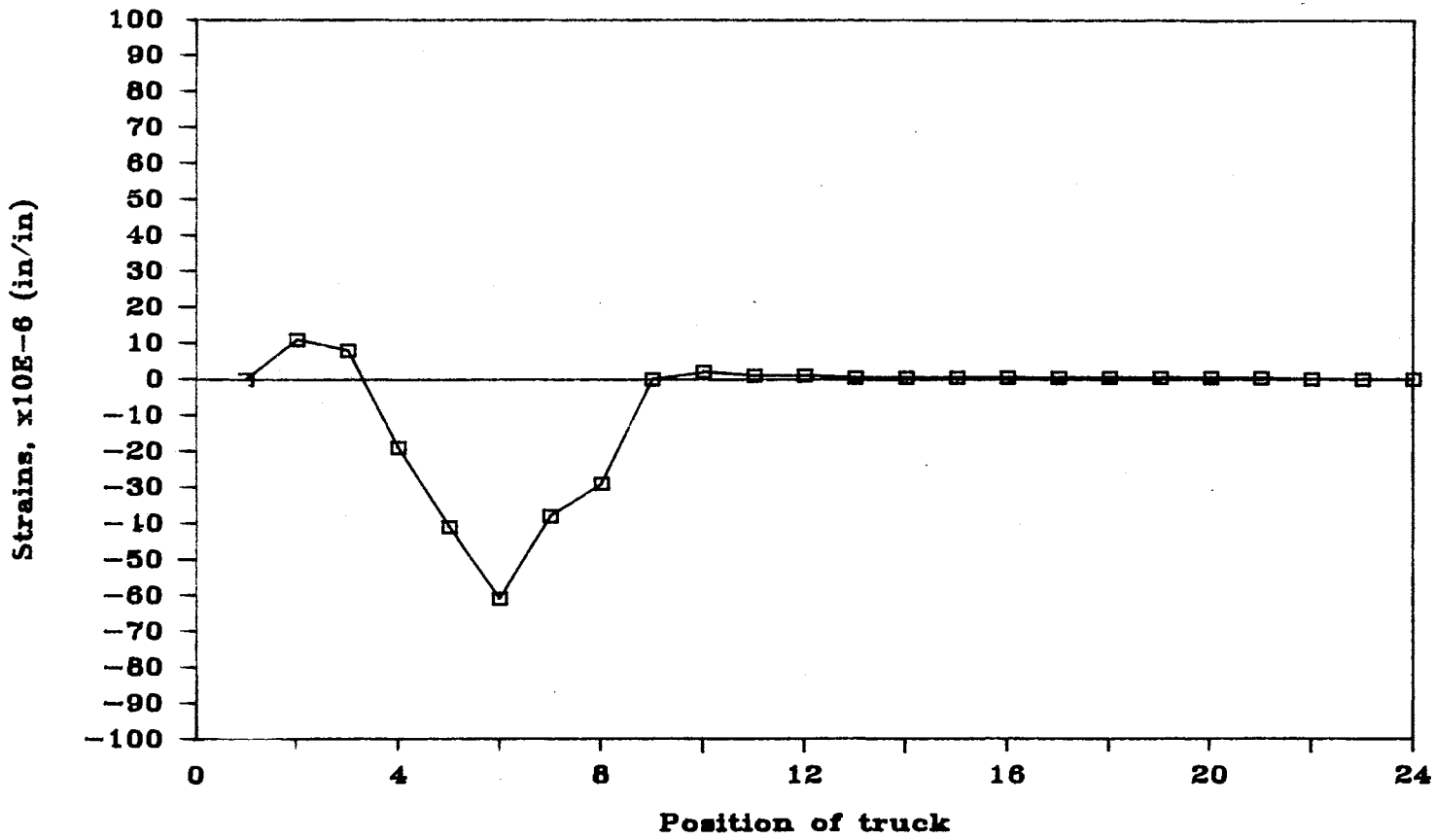

Figure 31. Strains for various lane loading positions, field instrumented exterior diaphragm, gage #3

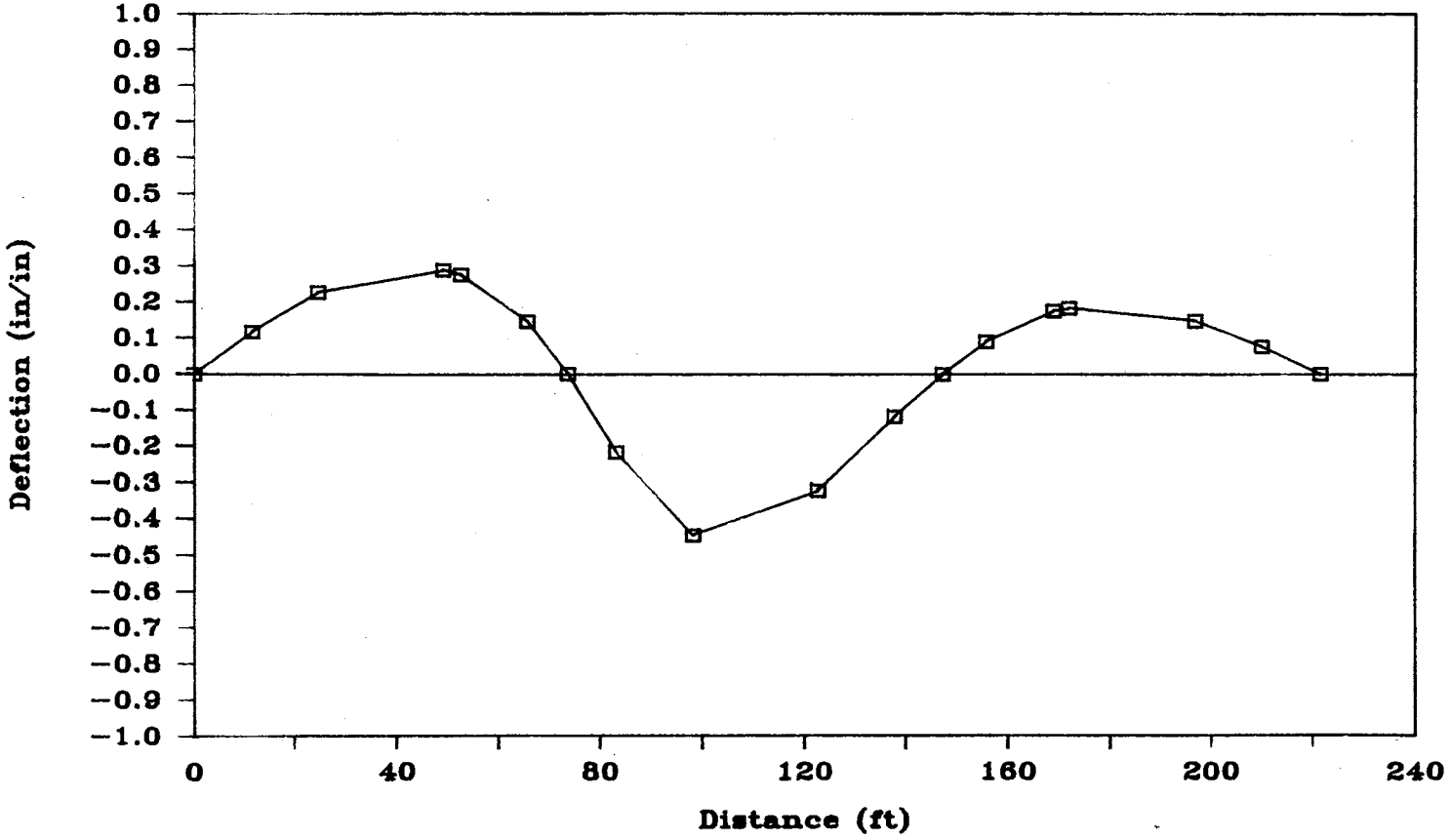

Figure 32. Deflected shape of the center girder obtained using the grid model, loading at position 5

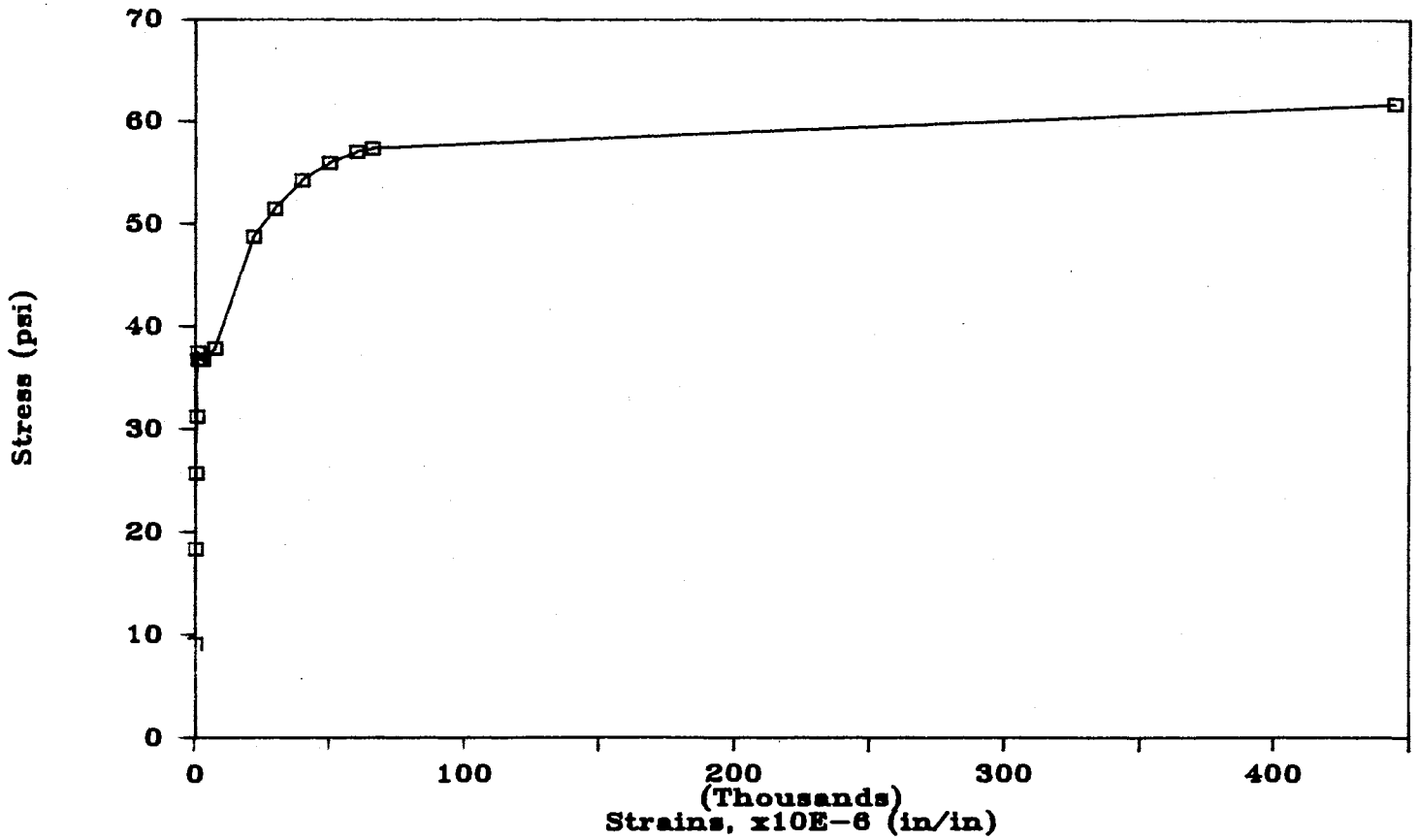

Figure 33. Stress versus strain curve for flange specimen 1

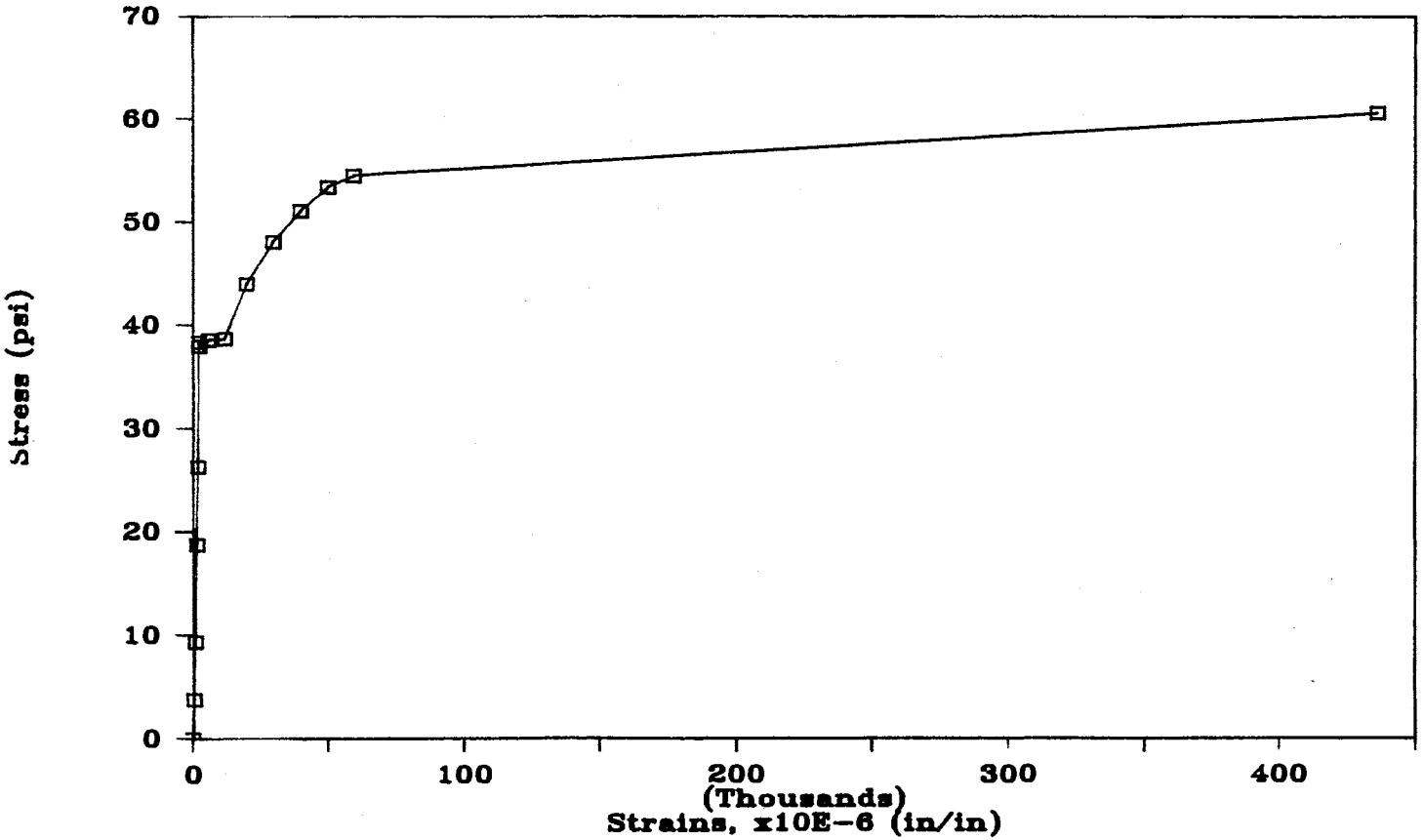

Figure 34. Stress versus strain curve for flange specimen 2

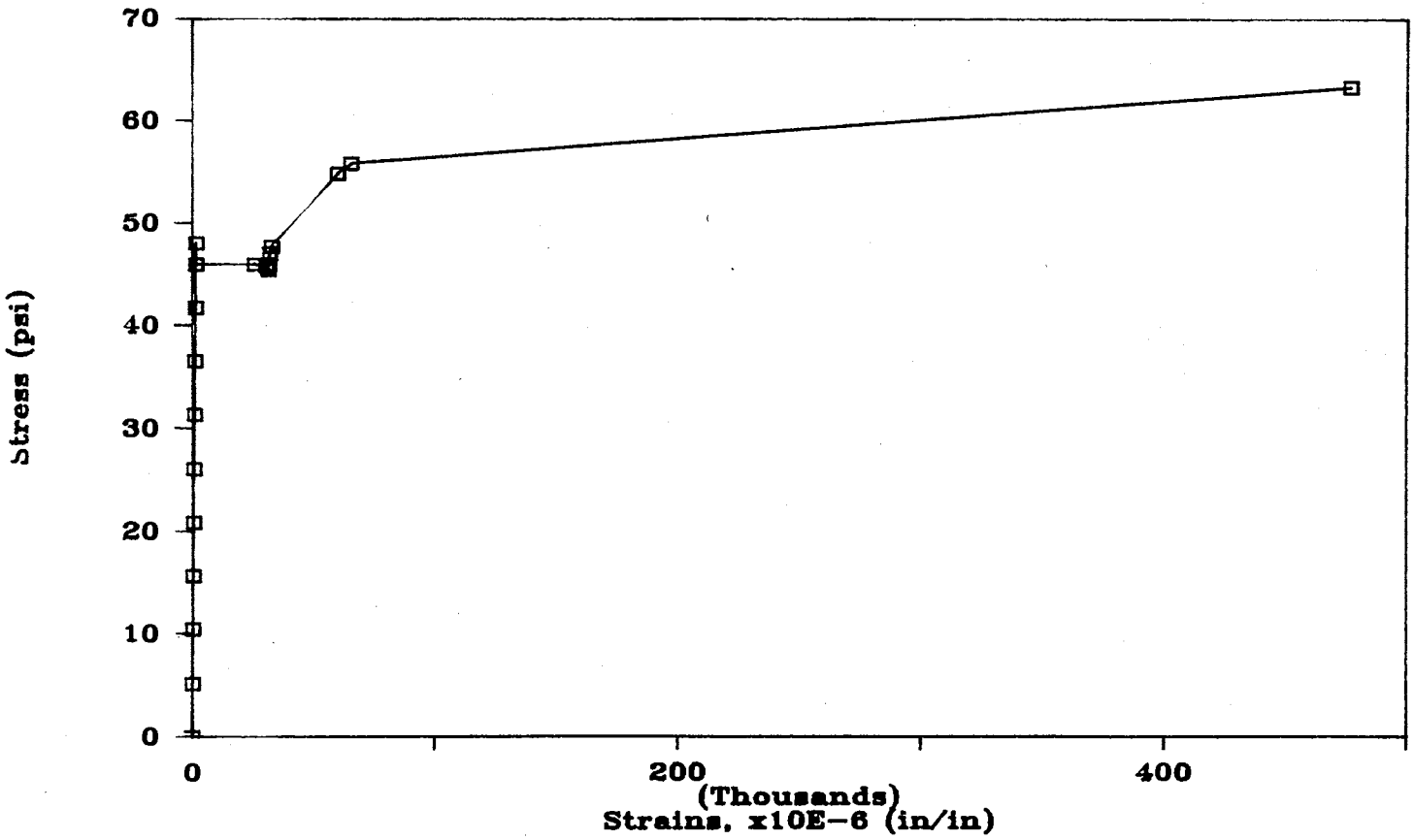

Figure 35. Stress versus strain curve for web specimen 1

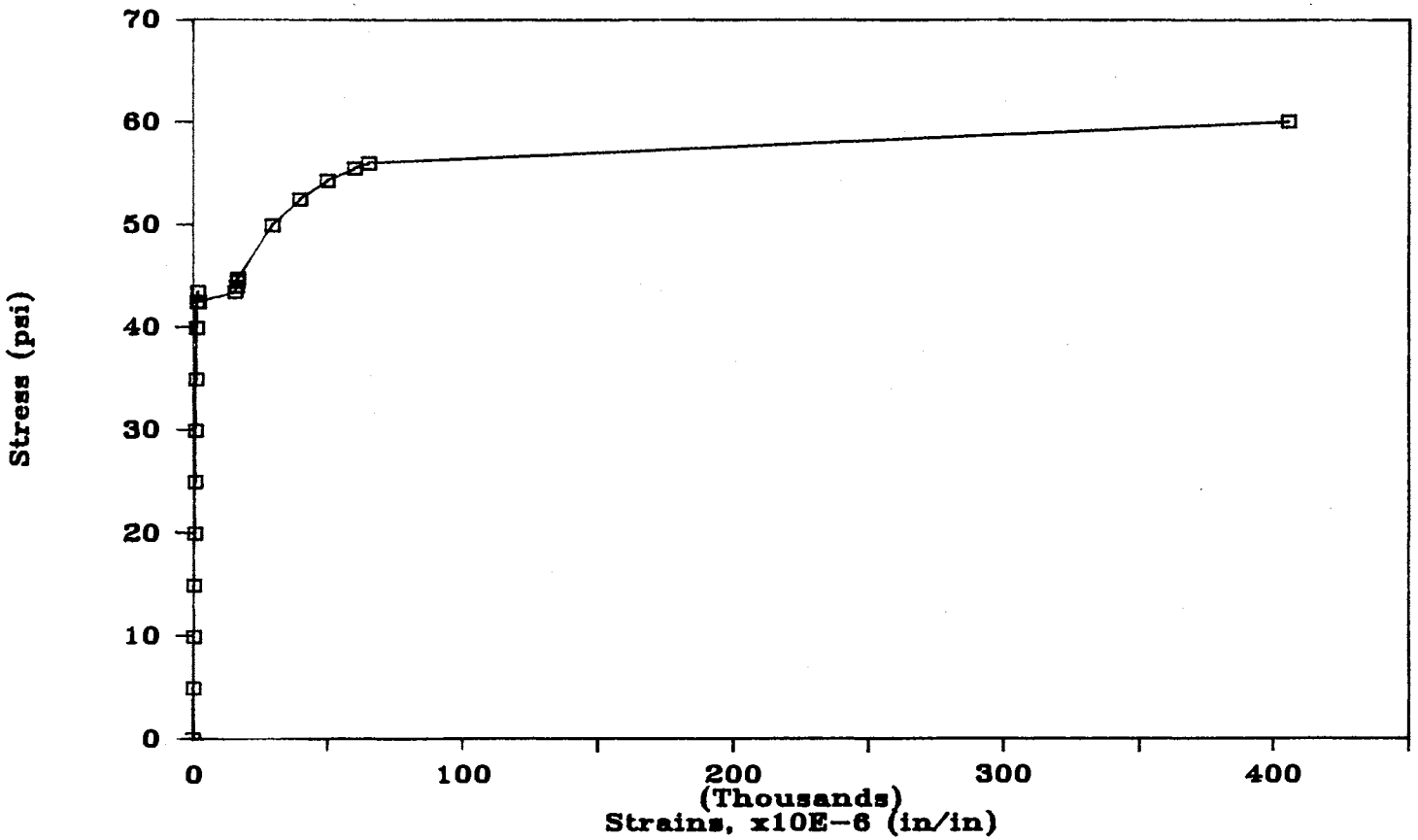

Figure 36. Stress versus strain curve for web specimen 2

VITA

Lim Kee Seong

Candidate for the Degree of

Master of Science

Thesis: FATIGUE DAMAGE TO STEEL BRIDGE DIAPHRAGMS, FIELD INVESTIGATION

Major Field: Civil Engineering

Biographical:

Personal Data: Born in Klang, Selangor, Malaysia, June 4, 1959, the son of Mr. and Mrs. Lim Kim Huay.

Education: Received Bachelor of Science in Civil Engineering from Oklahoma State University in May, 1987; completed requirements for the Master of Science degree at Oklahoma State University in May, 1989.

Professional Experience: Graduate Research Assistant, Department of Civil Engineering, Oklahoma State University, May, 1987 to Jan, 1989. Teaching Assistant, Department of Civil Engineering, Oklahoma State University, Jan, 1987 to May, 1987 and also from Aug, 1988 to Dec, 1988.